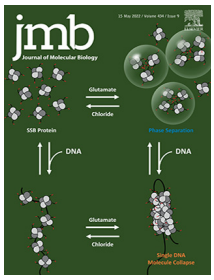

CNOT7 Outcompetes Its Paralog CNOT8 for Integration into The CCR4-NOT Complex

Patrick N. Stoney * **Akiko Yanagiya, Saori Nishijima and Tadashi Yamamoto** *

Cell Signal Unit, *Okinawa Institute of Science and Technology Graduate University, 1919-1 Tancha, Onna, Okinawa 904-0495, Japan*

Correspondence to Patrick N. Stoney and Tadashi Yamamoto: Fax: +81 98 966 1064. *patrick.stoney@oist.jp (P. N. Stoney), tadashi.yamamoto@oist.jp (T. Yamamoto)*
https://doi.org/10.1016/j.jmb.2022.167523
Edited by Moshe Yaniv

Abstract

The CCR4-NOT deadenylase complex is a major post-transcriptional regulator of eukaryotic gene expression. CNOT7 and CNOT8 are both vertebrate homologs of the yeast CCR4-NOT catalytic subunit Caf1. They are highly similar and are sometimes considered redundant, but *Cnot7* and *Cnot8* knockout mice exhibit different phenotypes, implying distinct physiological functions. In this study, we reveal a non-reciprocal effect of CNOT7 on CNOT8, in which CNOT8 protein is increased in the depletion of CNOT7 without corresponding changes in mRNA levels whereas CNOT7 is not affected by the loss of CNOT8. *Cnot8* mRNA may be bound by the CCR4-NOT complex, suggesting that CCR4-NOT might directly regulate CNOT8 expression. *Cnot8* mRNA is relatively unstable, but *Cnot7* knockdown did not stabilize *Cnot8* mRNA, nor did it increase translation. CNOT8 protein was also less stable than CNOT7. CNOT7 showed greater affinity than CNOT8 for the CCR4-NOT scaffold protein CNOT1 and was able to block CNOT8 from binding to CNOT1. Depletion of CNOT7 increased CNOT8 incorporation into the CCR4-NOT complex and stabilized CNOT8. These data suggest that CNOT7 is the dominant paralog in CCR4-NOT and that CNOT7 and CNOT8 protein stability is regulated in distinct ways.

Introduction

The level of mRNA expression in each cell is determined by the equilibrium between transcription and mRNA decay. The carbon catabolite repressor 4-negative on TATA-less (CCR4-NOT) complex is the major regulator of mRNA stability in eukaryotic cells and thus plays a central role in determining mRNA levels within the cell.[1] CCR4-NOT catalyzes the removal of the 3′ poly(A) tail, which is considered the first and rate-limiting step in mRNA decay.[2] In addition to regulating mRNA stability, there is evidence that CCR4-NOT controls other aspects of the mRNA life cycle, including transcription[3] and translation.[4] In mammals, deletion of several of the subunits of CCR4-NOT is embryonic lethal,[5–7] and mutations in CCR4-NOT subunits have been linked to resistance to obesity,[7–8] diabetes,[9] and neurodevelopmental disorders such as autism.[10–11] The importance of CCR4-NOT in cellular homeostasis and its relevance to human disease make it vital to understand the structure and function of the complex and its subunits.

The CCR4-NOT complex is highly conserved in eukaryotes. The yeast CCR4-NOT complex contains two catalytic deadenylase subunits, Caf1 and Ccr4,[1] but each deadenylase subunit has been duplicated in vertebrates. The vertebrate orthologs of yeast Caf1 are CNOT7 (CAF1a) and CNOT8 (CAF1b, also known as POP2). CNOT7 and CNOT8 serve a catalytic role in the CCR4-NOT

complex, but also a scaffolding role in recruiting the other deadenylase subunits, CNOT6 (CCR4a) and CNOT6L (CCR4b), to the complex.[12] In higher eukaryotes, CNOT7/8 was believed to be the dominant deadenylase subunit of CCR4-NOT,[13] although more recent data suggests that both CNOT7/8 and CNOT6/6L contribute to mRNA degradation.[14] CNOT7/8 and CNOT6/6L may differ in their specificity, as human CNOT6/6L was found to degrade poly(A) RNA bound by poly(A)-binding protein (PABP), whereas CNOT7/8 could only degrade PABP-free poly(A).[15] A recent study found that binding to a mutant CNOT6 lacking nuclease activity enhanced the deadenylase activity of CNOT7,[16] suggesting a more cooperative mode of action than previously thought.

The reason why CNOT7 and CNOT8 exist in vertebrates is not clear. As paralogs arising from gene duplication, they are highly similar proteins (75% identical amino acid sequences), and current evidence suggests that CNOT7 and CNOT8 are partly redundant and regulate some of the same mRNA targets.[17] However, whole-body *Cnot8* knockout (*Cnot8*-KO) in mouse is embryonic lethal at around E9.0,[6] whereas *Cnot7*-KO mice are viable but display various phenotypes, including defective spermatogenesis,[3,18] increased bone density[19] and resistance to obesity.[8] Since *Cnot7* and *Cnot8* null mutant mice have different phenotypes, it appears that each protein has distinct functions and in certain cases, each paralog cannot compensate for the other.

In vitro experiments using recombinant proteins suggested that CNOT8 may be a more efficient deadenylase than CNOT7, but with lower specificity for poly(A).[20] However, binding to CCR4-NOT increases both activity and specificity.[14] Co-immunoprecipitation followed by mass spectrometry identified 199 proteins immunoprecipitating with human CNOT7, but only 46 with CNOT8.[12] Excluding CCR4-NOT subunits, only 19 proteins were common to both CNOT7 and CNOT8, implying functional divergence. More recently, analysis of cytosolic RNA granules using BioID, which can detect low-affinity and transient interactions, did not show such large differences between CNOT7 and CNOT8.[21] Individual knockdown of CNOT7 or CNOT8 in MCF7 breast cancer cells had little effect on mRNA expression, implying redundancy, but both subunits were required for maximal proliferation,[17] suggesting that their functions do not overlap completely. Tethering assays in *Xenopus* oocytes suggest that both CNOT7 and CNOT8 could repress translation independently of deadenylation and mRNA stability.[4,22] Moreover, CNOT7 has been shown to regulate transcription via binding to nuclear receptors,[3,23] but it is not known if this is also the case for CNOT8.

In this study, we show that CNOT8 protein is elevated in the absence of CNOT7 as a result of increased protein stability. CNOT8 stability is dependent on binding to CNOT1, whereas CNOT7 is inherently stable, and CNOT7 binds preferentially to CNOT1, preventing the incorporation of CNOT8 into CCR4-NOT. The data presented in this study suggest that CNOT7 is likely to be the dominant paralog in the CCR4-NOT complex, excluding the less stable CNOT8.

Results

Depletion of CNOT7 protein increases CNOT8 protein

CNOT7 and CNOT8 bind to the same site of CNOT1 in a mutually exclusive manner[12,24] and are thought to regulate at least some of the same mRNA targets,[17] and so the two paralogs may compete with one another or may compensate for loss of the other. We investigated whether the expression level of each subunit is influenced by the other using knockout mice. CNOT8 levels were compared by western blotting in various tissues from male wild-type and *Cnot7*-KO mice at 13 weeks of age. Expression of CNOT7 and CNOT8 protein differed between tissues, but CNOT8 was consistently increased in all *Cnot7*-KO tissues relative to wild-type (Figure 1(A)). Short-term depletion of CNOT7 in N2A mouse neuroblastoma cells using siRNA also increased CNOT8 protein (Figure 1(B)). However, *Cnot8* mRNA levels were not affected by CNOT7 depletion (Figure 1(C)). These data suggest that loss of CNOT7 acts post-transcriptionally to increase CNOT8 protein expression. Loss of CNOT7 did not affect protein expression of all CCR4-NOT subunits, as CNOT3 expression was unaltered by *Cnot7* knockdown (Figure 1(B)).

As whole-body *Cnot8* deletion (*Cnot8*-KO) in mice is embryonic lethal,[6] the effect of CNOT8 loss *in vivo* was investigated using conditional knockout mice in which CNOT8 was deleted using Cre driven by the *Camk2a* promoter.[25] *Camk2a* is a marker of a large population of excitatory forebrain neurons,[26] whose expression begins in late embryogenesis,[27] after the stage at which *Cnot8*-KO mice die. Conditional *Cnot8* mutants (*Cnot8*-cKO) were viable with no obvious phenotypes. In the hippocampus of adult *Cnot8*-cKO mice, CNOT8 protein was reduced by 85% (Figure 1(D)), but CNOT7 protein expression was unaffected. This suggests that loss of CNOT8 does not affect CNOT7, in contrast to the effect of CNOT7 loss to increase CNOT8. The increase in CNOT8 could be reproduced in cell lines using siRNA to deplete CNOT7 and therefore we used this approach to investigate the underlying mechanism by which CNOT7 depletion increases CNOT8 protein.

CNOT8 translation is not increased by CNOT7 depletion

Evidence from tethering assays suggests that CNOT7 (and CNOT8) may regulate translation

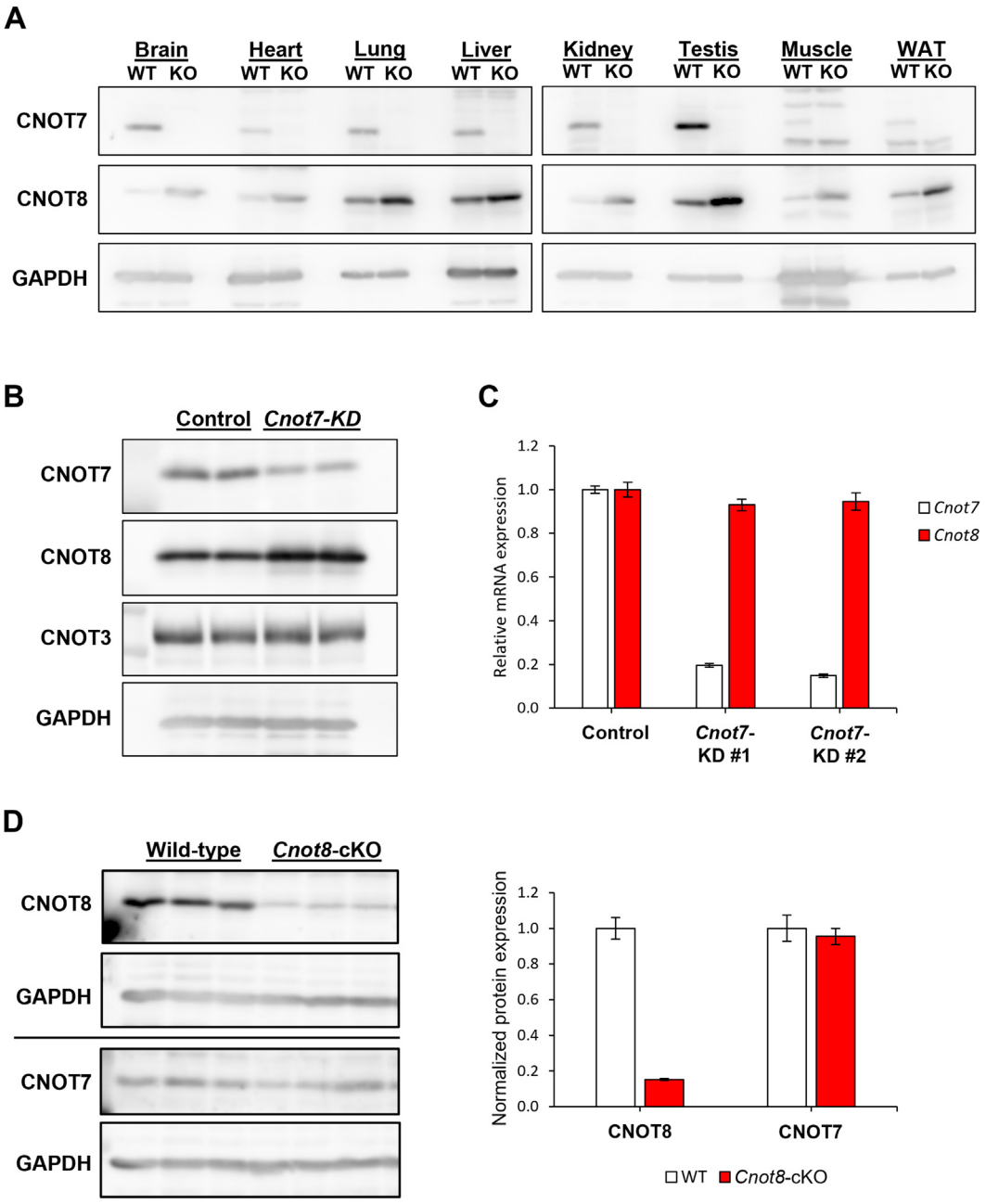

Figure 1. Depletion of CNOT7 protein increases expression of its paralog CNOT8. (A) CNOT8 protein expression was increased in tissues from *Cnot7*-KO mice (13-week-old male) compared to wild-type (WT) littermates. (B) CNOT8 protein expression was also increased in N2A cells following depletion of CNOT7 using siRNA. Other subunits, such as CNOT3, were unaffected. (C) *Cnot7* knockdown (*Cnot7*-KD; white) in N2A cells using siRNA did not affect *Cnot8* mRNA (red) expression, as measured by qPCR. The results of two different siRNAs targeting *Cnot7* are shown. (D) CNOT7 protein expression is unaffected by conditional *Cnot8* deletion in excitatory neurons in the hippocampus. Quantification of CNOT7 and CNOT8 expression in WT (white) or *Cnot8*-cKO (red) hippocampi by densitometry is shown on the right. The values shown in graphs represent the mean; error bars show the standard error of the mean (SEM).

independently of deadenylation via binding to the encoding mRNA.[4] Therefore, if CNOT7 directly affects translation of CNOT8, *Cnot8* mRNA should interact with CNOT7-containing CCR4-NOT complexes. To investigate whether *Cnot8* mRNA might be bound by the CCR4-NOT complex, an antibody against CNOT3 was used to immunoprecipitate (IP) the whole complex, together with bound mRNAs, as previously published by our laboratory,[28] from N2A cell lysates. RNA was extracted

from the IP fraction and input samples and CCR4-NOT-associated mRNAs detected using qPCR. Ribonucleoprotein-immunoprecipitation (RIP) assays detected mRNAs encoding all the CCR4-NOT deadenylase subunits (Figure 2(A)). Co-immunoprecipitation of these mRNAs was specific to the CNOT3 antibody as no mRNA was detected in RIP assays using a control mouse IgG. Relative to input expression, more *Cnot8* mRNA co-immunoprecipitated with CNOT3 than the mRNAs encoding the other deadenylase subunits (1% of input for *Cnot8* mRNA; 0.10% for *Cnot6*; 0.32% for *Cnot6l*; 0.43% for *Cnot7*). Following *Cnot7* knockdown in N2A cells (*Cnot7*-KD), co-immunoprecipitation of *Cnot6l* and *Cnot8* mRNAs with CNOT3 appeared to be reduced (69% reduction of both *Cnot6l* and *Cnot8*; Figure 2(A)), although it did not reach statistical significance. This raises the possibility that the binding of *Cnot6l* and *Cnot8* mRNA by CCR4-NOT may be influenced by CNOT7, directly or indirectly, and that the increased CNOT8 in *Cnot7*-KD cells does not completely compensate for loss of CNOT7 in this case. It cannot be ruled out that mRNAs are associated with CNOT3 via interactions with non-CCR4-NOT proteins, such as translating ribosomes,[29] although there is currently no evidence that loss of CNOT7 or CNOT8 affects the interaction of CNOT3 with other proteins. Steady-state levels of *Cnot6l* and *Cnot8* mRNA in *Cnot7*-KD cells were not significantly different to control cells, as determined by qPCR using cDNA from input samples (Figure 2(A)). However,

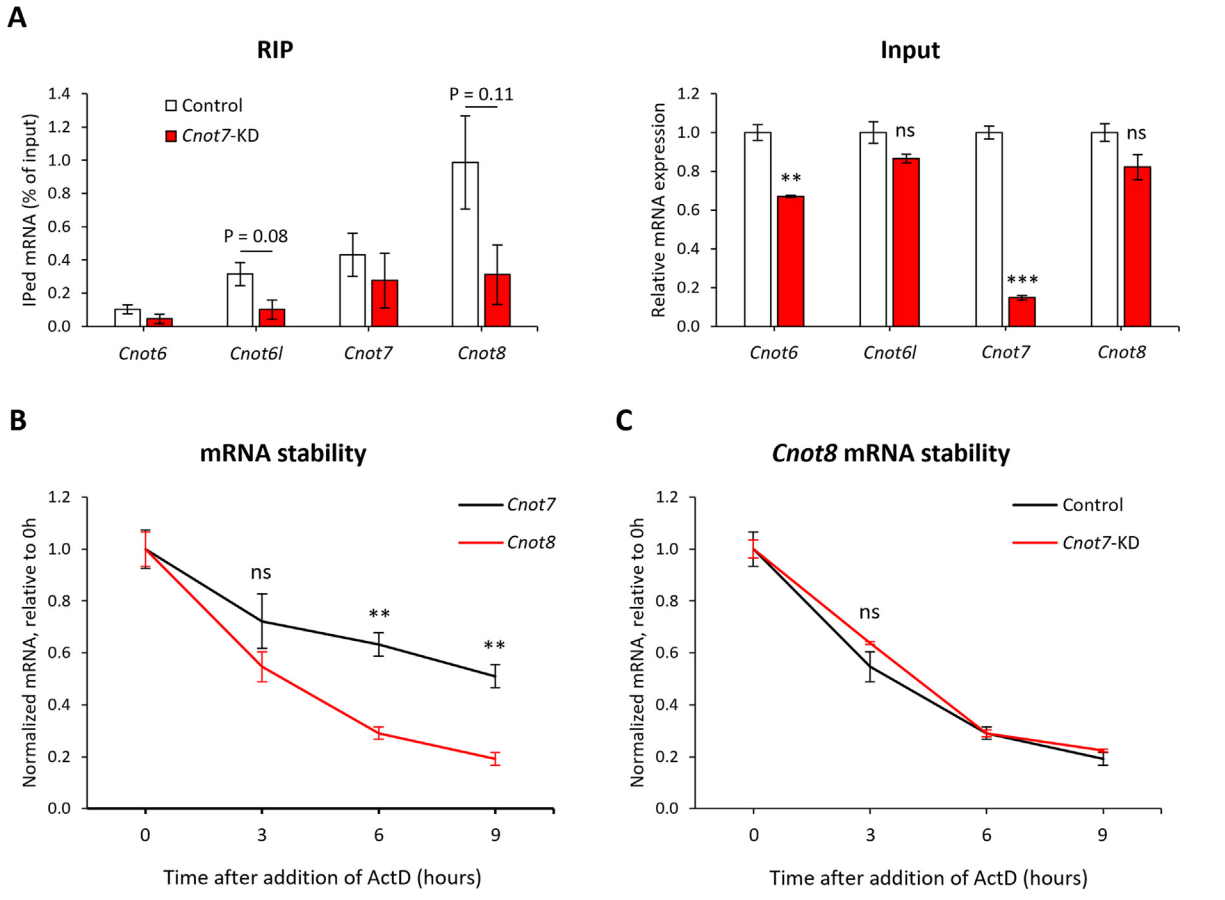

Figure 2. *Cnot8* mRNA is unstable, but its stability is unaffected by CNOT7 depletion. (A) Ribonucleoprotein-immunoprecipitation (RIP) assays using an anti-CNOT3 antibody suggested that *Cnot8* mRNA might be bound by the CCR4-NOT complex in N2A cells. Co-immunoprecipitation of *Cnot6l* and *Cnot8* mRNA with CNOT3 appeared reduced in *Cnot7*-KD cells. The mean percentage of mRNA bound to CNOT3 relative to input expression in control (white) or *Cnot7*-KD (red) cells is shown. Parallel RIP assays using a control mouse IgG did not detect non-specific mRNA binding and are therefore not shown. Input levels of *Cnot6l* and *Cnot8* mRNA were unaffected by *Cnot7* knockdown. Mean mRNA expression relative to control siRNA-treated cells is shown. (B) Inhibition of transcription using actinomycin D (ActD) suggested that *Cnot8* mRNA (red) is significantly less stable than *Cnot7* mRNA (black). (C) *Cnot8* mRNA stability did not differ between control (black) and *Cnot7*-KD (red) cells. Graphs in (B) and (C) show normalized mean mRNA expression at each timepoint relative to expression at 0 h. Error bars in all graphs show SEM. ns, not significant; **, $p < 0.01$; ***, $p < 0.001$; Student's t-test.

Cnot6 mRNA expression was reduced in *Cnot7*-KD N2A cells (33% reduction; $P < 0.01$).

Since *Cnot8* mRNA could be bound by CCR4-NOT, CNOT7 depletion could affect its stability or turnover rate, even if steady-state mRNA levels are not altered. To measure mRNA stability, N2A cells were treated with a transcriptional inhibitor, actinomycin D (ActD; 10 μg/ml), and samples were collected for qPCR after 0, 3, 6 and 9 hours of treatment. Consistent with it being a potential CCR4-NOT target, *Cnot8* mRNA (half-life = 3.5 hours) was significantly less stable than *Cnot7* (mRNA half-life = 9 hours; $P < 0.01$ from 6 h after addition of ActD; Figure 2(B)). However, CNOT7 depletion in N2A cells using siRNA did not affect the stability of *Cnot8* mRNA (Figure 2(C)). These data suggest that the increased CNOT8 protein in CNOT7-depleted cells does not result from stabilization of *Cnot8* mRNA.

CCR4-NOT is recruited to its mRNA targets by a number of RNA-binding proteins that bind to sites mainly located in the 3′ untranslated region (UTR).[30] Comparative analysis of the *Cnot8* 3′UTR using the ECR Browser (ecrbrowser.dcode.org[31]) identified two regions that were highly conserved in mammals (Figure S1), each containing several potential binding sites for proteins known to recruit CCR4-NOT to its targets (Figure 3(A); Figure S2). Several putative microRNA binding sites were also identified in these conserved regions using TargetScan (targetscan.org/mmu_71[32]).

Cnot8 mRNA stability was unaffected by *Cnot7*-KD, but CNOT7 could suppress translation of CNOT8 protein without affecting mRNA stability.[4,22] To assess the effect of CNOT7 depletion on the translational efficiency of *Cnot8* mRNA, the full *Cnot8* 3′UTR, ECR1 or ECR2 (Figure 3(A)) were cloned into a modified pGL3 vector (Promega)[8] downstream of a firefly luciferase reporter gene (*FLuc*). 24 hours after siRNA transfection, control or *Cnot7*-KD N2A cells were transfected with the *Cnot8* 3′UTR reporter plasmids, together with renilla luciferase-expressing pRL-TK. The following day, the cells were lysed and luciferase activity measured. The inclusion of the full *Cnot8* 3′UTR increased luciferase activity (52% increase over Δ3′UTR controls; $P < 0.001$; Figure 3(B)). Luciferase expression was not increased in *Cnot7*-KD cells, suggesting that translation was not increased by CNOT7 depletion. In fact, luciferase levels were reduced in *Cnot7*-KD compared to control siRNA-transfected cells (28% reduction; $P < 0.05$). ECR1 alone reproduced the effects of the full *Cnot8* 3′UTR on luciferase activity, whereas ECR2 had no effect in this context. *FLuc-ECR1* mRNA was increased relative to *FLuc-Δ3′UTR* mRNA and *FLuc-ECR1* mRNA expression was not different in *Cnot7*-KD cells compared to controls (Figure S3(C)), suggesting that the decreased luciferase activity in *Cnot7*-KD (Figure 3(B)) was due to reduced translation. These data suggest that elements within ECR1 of the *Cnot8* 3′UTR may regulate translation, but CNOT7 depletion does not increase translation of *Cnot8* mRNA via its 3′UTR.

The open reading frame (ORF) of *Cnot8* could also contribute to regulating translation. If translation of *Cnot8* mRNA is enhanced, the number of ribosomes bound to *Cnot8* mRNA should increase. To examine translational efficiency of endogenous *Cnot8* mRNA, including the ORF, lysates from control or *Cnot7*-KD N2A cells were fractionated using a sucrose density gradient to separate mRNAs bound to single ribosomes (monosomes), and light and heavy polysomes (Figure S3(F)). Total RNA was extracted from all fractions and *Cnot8* mRNA was quantified in each fraction by qPCR. No significant differences were observed in the distribution of *Cnot8* mRNA following polysome fractionation using control and *Cnot7*-KD cells (Figure 3(C)). This indicates that ribosome occupancy (and therefore translational efficiency) on *Cnot8* mRNA is not altered in CNOT7-depleted cells. Together, the results of the luciferase assays and polysome profiling suggest that the increased CNOT8 protein in CNOT7-depleted cells does not result from increased translation from *Cnot8* mRNA.

CNOT8 protein is less stable than CNOT7

Since *Cnot8* mRNA stability and translation were not increased in *Cnot7*-KD cells, the elevated CNOT8 in the absence of CNOT7 could arise from increased stability of CNOT8 protein. To

Figure 3. CNOT7 depletion does not increase translation of *Cnot8* mRNA. (A) The 3′UTR of *Cnot8* mRNA contains several highly conserved potential binding sites for proteins known to recruit CCR4-NOT to its targets. The annotated sequences of evolutionarily conserved region 1 (ECR1) and 2 (ECR2) are shown in Figure S2. (B) Luciferase assays using constructs containing ECR1, ECR2 or the full mouse *Cnot8* 3′UTR suggested that elements within ECR1 could affect *Cnot8* translation, but CNOT7 depletion did not increase translation via the *Cnot8* 3′UTR. The graph shows firefly luciferase activity relative to control cells transfected with the reporter construct containing no *Cnot8* 3′UTR (Δ3′UTR) in control (white) and *Cnot7*-KD (red) cells; error bars show SEM. Data were analysed by ANOVA followed by Tukey's *post hoc* tests. (C) Polysome fractionation did not show any differences in the distribution of *Cnot8* mRNA in control (black) and *Cnot7*-KD (red) cells, suggesting that translation was not increased. Normalized *Cnot8* mRNA expression in each fraction relative to total mRNA is shown; error bars show SEM. ns, not significant; *, $p < 0.05$; ***, $p < 0.001$.

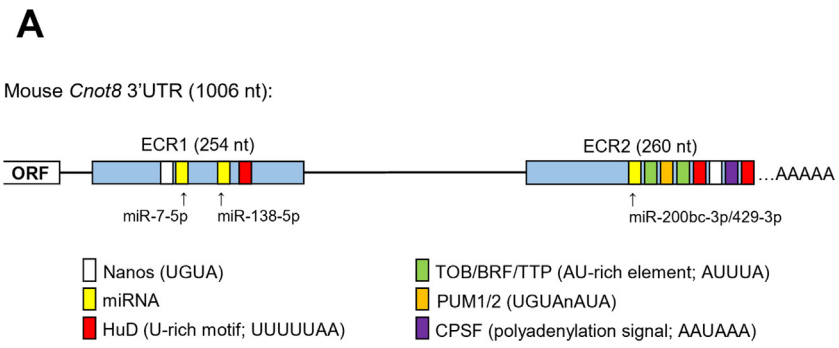
A
Mouse Cnot8 3'UTR (1006 nt):
ECR1 (254 nt)
ECR2 (260 nt)
ORF
...AAAAA
miR-7-5p
miR-138-5p
miR-200bc-3p/429-3p
Nanos (UGUA)
miRNA
HuD (U-rich motif; UUUUUAA)
TOB/BRF/TTP (AU-rich element; AUUUA)
PUM1/2 (UGUAnAUA)
CPSF (polyadenylation signal; AAUAAA)

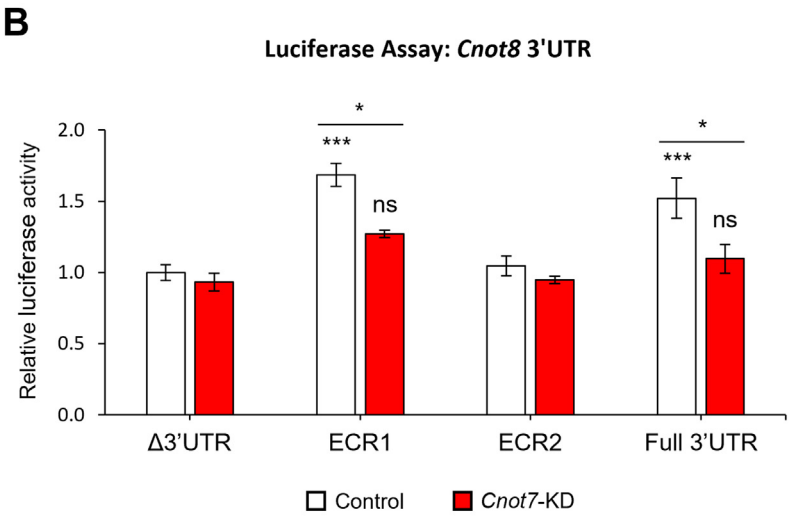
B
Luciferase Assay: Cnot8 3'UTR
Relative luciferase activity
2.0
1.5
1.0
0.5
0.0
*
***
ns
*
***
ns
Δ3'UTR
ECR1
ECR2
Full 3'UTR
Control
Cnot7-KD

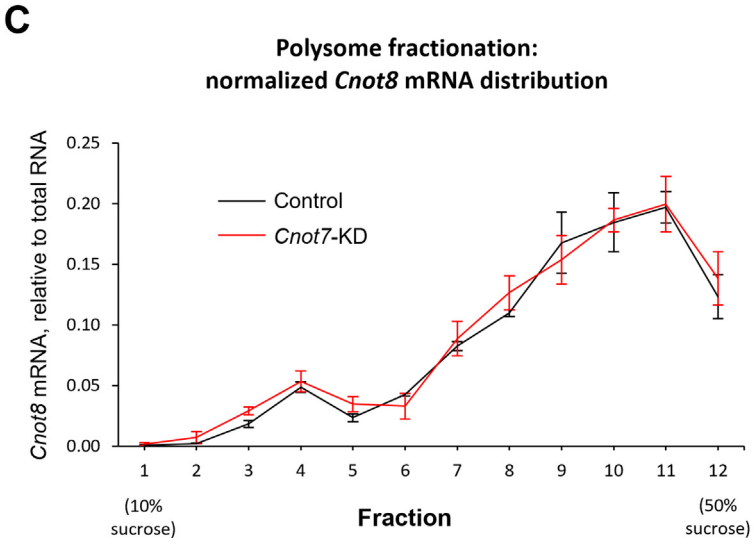
C
Polysome fractionation:
normalized Cnot8 mRNA distribution
Cnot8 mRNA, relative to total RNA
0.25
0.20
0.15
0.10
0.05
0.00
Control
Cnot7-KD
1
2
3
4
5
6
7
8
9
10
11
12
(10% sucrose)
Fraction
(50% sucrose)

investigate this, protein synthesis was blocked in N2A cells using the translational inhibitor cycloheximide (CHX) to monitor protein degradation. Cells were treated with 25 μM or 50 μM CHX and lysed at 0, 14 and 24 hours for analysis by western blotting. After 24 hours of treatment with 25 μM CHX, CNOT8 protein was decreased by 55% (Figure 4(A)). In contrast, CNOT7 protein levels remained almost constant (105 ± 12% of starting expression at 24 h after addition of CHX), suggesting that it is relatively stable. β-catenin is rapidly degraded by the proteasome and was used as a positive control to confirm CHX activity. The proteasome inhibitor MG132 (10 μM) blocked degradation of CNOT8 in CHX-treated N2A cells (44% decrease in CHX-treated cells versus 10% decrease in cells treated with CHX + MG132; P = 0.006; Figure 4(B)), implying the possible involvement of the ubiquitin–proteasome pathway in the degradation of CNOT8 protein. These data demonstrate that, despite the high similarity in their amino acid sequences, CNOT8 is less stable than CNOT7 and that it may be actively degraded by the proteasome.

CNOT7 depletion stabilizes CNOT8 and increases CNOT8 integration into CCR4-NOT

To determine whether stability of CNOT8 protein is dependent on CNOT7 expression, N2A cells were transfected with control or *Cnot7* siRNA and then 48 hours later were treated with 25 μM CHX for 0, 14 and 24 hours. As previously shown (Figure 1(A), (B)), CNOT8 protein was increased in *Cnot7*-KD cells, but it was also more stable; in the first 14 hours of CHX treatment, CNOT8 decreased by over 50% in control cells, but only by 9% in CNOT7-depleted cells (Figure 5(A)). Degradation of β-catenin was similar between control and CNOT7-depleted cells. These data suggest that the rate of CNOT8 degradation is slowed by depletion of CNOT7.

CNOT7 and CNOT8 bind to the same region of the MIF4G domain of CNOT1[24] in a mutually exclusive manner.[12] Therefore, loss of CNOT7 could allow increased binding of CNOT8 to the CCR4-NOT complex, which may protect it from degradation and increase its stability. CNOT7 was depleted in N2A cells using siRNA and 48 hours later, the whole CCR4-NOT complex was

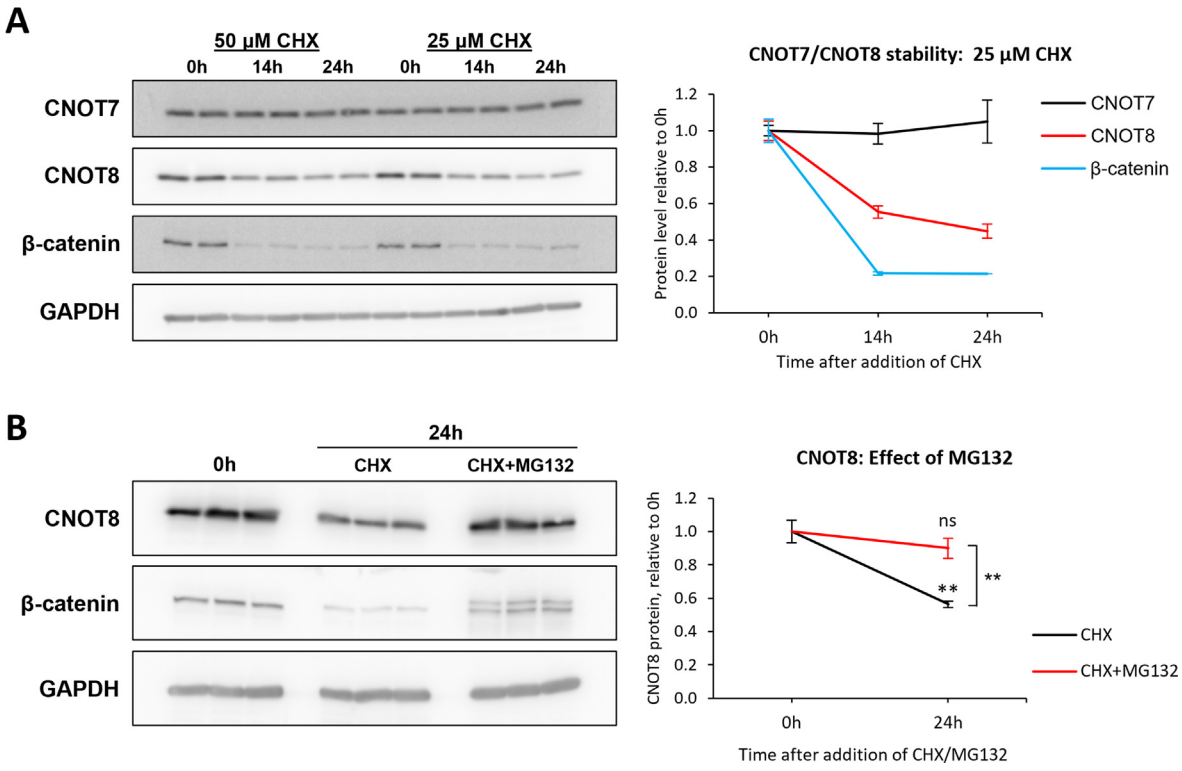

Figure 4. CNOT8 protein is less stable than CNOT7 protein. (A) In N2A cells treated with the translation inhibitor cycloheximide (CHX), CNOT8 protein decreased by more than 50% over 24 hours, while in the same cells CNOT7 protein remained constant. Results were similar for 50 μM and 25 μM CHX. Quantification of CNOT7 (black), CNOT8 (red) and β-catenin (blue) protein expression in 25 μM CHX-treated cells by densitometry is shown on the right side. (B) Addition of the proteasome inhibitor MG132 (10 μM) blocked degradation of CNOT8 in CHX-treated cells. CNOT8 protein levels are shown in the absence (black) or presence (red) of MG132. β-catenin was used as a control for both CHX and MG132 activity. The graphs show mean protein expression relative to 0 h, normalized to GAPDH; error bars show SEM. **, $p < 0.01$, Student's t-test.

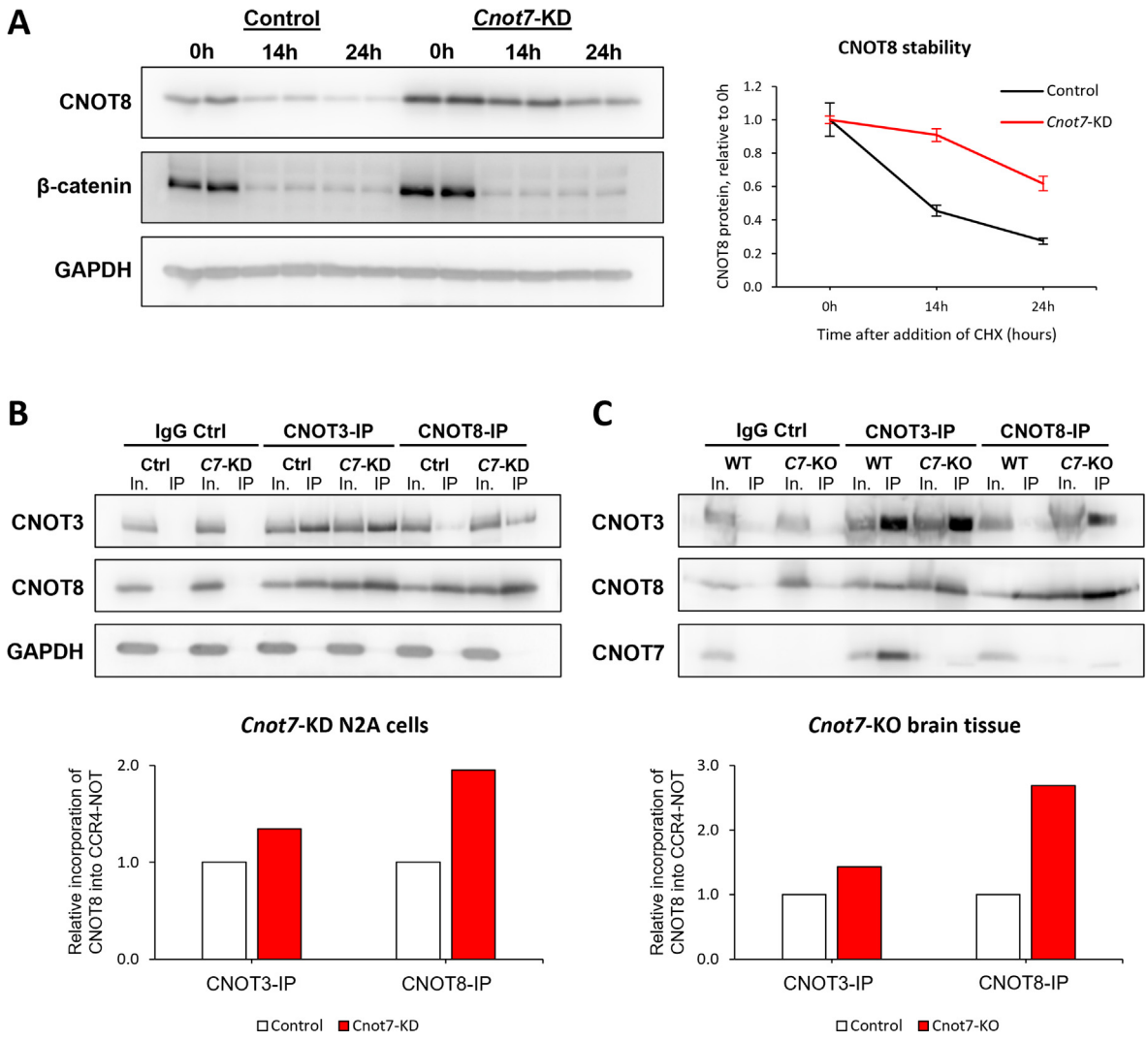

Figure 5. CNOT7 depletion increases CNOT8 integration into the CCR4-NOT complex. (A) CNOT7 depletion in N2A cells before cycloheximide treatment (CHX, 25 μM) increased the stability of CNOT8 protein. The graph shows mean protein expression in control (black) and *Cnot7*-KD (red) cells relative to 0 h for each condition, normalized to GAPDH; error bars show SEM. (B) *Cnot7* knockdown (C7-KD) in N2A cells increased the amount of CNOT8 co-immunoprecipitating with CNOT3 (CNOT3-IP). More CNOT3 also co-immunoprecipitated with CNOT8 (CNOT8-IP). (C) Similar results were obtained by CNOT3-IP and CNOT8-IP using forebrain tissue lysates from wild-type and *Cnot7*-KO littermates (12-week-old female). For (B) and (C), the interaction between CNOT8 and CCR4-NOT has been quantified from the western blots. Values of the co-IPed protein in *Cnot7*-KD cells or *Cnot7*-KO tissue were normalized to the IPed protein level and expressed relative to controls.

immunoprecipitated using an anti-CNOT3 antibody. Input levels of CNOT3 were not different between control and *Cnot7*-KD cells, but CNOT8 was increased in CNOT3-IP samples from CNOT7-depleted cells (34% increase in CNOT8; Figure 5(B)), suggesting a greater association between CCR4-NOT and CNOT8 in the absence of CNOT7. IP was also performed using an antibody against CNOT8. In control cells, expressing normal levels of CNOT7, co-IP of CNOT3 with CNOT8 was almost undetectable, but CNOT7 depletion increased CNOT3 levels in CNOT8-IP samples (96% increase in CNOT3; Figure 5(B)). CNOT3- and CNOT8-IP using tissue lysates from wild-type and *Cnot7*-KO mouse forebrain also showed increased co-immunoprecipitation of CNOT3 and CNOT8 in the absence of CNOT7 (43% increase in CNOT8 in CNOT3-IP; 169% increase in CNOT3 in CNOT8-IP; Figure 5(C)). Together, these data indicate that CNOT8 incorporation into the CCR4-NOT complex is increased when CNOT7 is reduced.

CNOT8 is stabilized by integration into the CCR4-NOT complex

We hypothesized that integration of CNOT7 and CNOT8 into the CCR4-NOT complex may protect them from degradation. To investigate this, N2A cells were transfected with FLAG-tagged wild-type or M141A mutant CNOT7/8, which cannot bind to the MIF4G domain of CNOT1 (Figure S4;[22,24]), then treated the cells with CHX to assess protein stability. After 24 hours of CHX treatment, FLAG-tagged wild-type CNOT8 was reduced by 50%, but FLAG-CNOT8-M141A was reduced by 72% (P = 0.018; Figure 6(A)) and was much less stable than endogenous CNOT8. β-catenin degradation was similar in both groups. Therefore, stability of CNOT8 is likely to be increased by its interaction with CNOT1.

In contrast to CNOT8, the stability of CNOT7-M141A in CHX-treated cells was similar to wild-type CNOT7 (Figure 6(B)). CHX activity was confirmed by β-catenin, whose degradation was consistent in each set of samples and was similar to FLAG-CNOT8-transfected samples. This implies that the difference in protein stability between CNOT7 and CNOT8 is not only due to binding to the CCR4-NOT complex, and additional regulation is present. That is, despite their similarity, their stability is likely to be regulated by different mechanisms.

The interaction between CNOT8 and CCR4-NOT was increased in CNOT7-depleted cells and this suggested that CNOT7 excludes CNOT8 from the complex. To investigate the competition between CNOT7 and CNOT8 for binding to CNOT1, recombinant FLAG-tagged human CNOT1-MIF4G domain (FLAG-CNOT1-MIF4G; 100 ng/reaction) was combined *in vitro* with an excess of recombinant human CNOT7 and CNOT8 (rCNOT7/8; 200 ng/reaction). Both rCNOT7 and rCNOT8 were able to bind FLAG-CNOT1-MIF4G in the absence of the other paralog (Figure 6(C)). When both rCNOT7 and rCNOT8 were incubated with FLAG-CNOT1-MIF4G, the interaction between CNOT7 and CNOT1-MIF4G appeared identical to when CNOT7 alone was present. In contrast, the presence of CNOT7 drastically reduced CNOT8 binding to FLAG-CNOT1-MIF4G. This suggests that CNOT7 binds to the MIF4G domain of CNOT1 with higher affinity than CNOT8 and can completely exclude CNOT8 from binding to CNOT1. Together with the data previously described (Figure 5), this indicates that CNOT7 is likely to be the dominant paralog in the CCR4-NOT complex.

In vivo, the ability of CNOT7 to exclude CNOT8 from the CCR4-NOT complex may be affected by the ratio of CNOT7 and CNOT8 in the cell. The amount of each protein in N2A cell lysates (6.3 μg per lane) was estimated by comparison to a range of standards made from recombinant human CNOT7 and CNOT8 (Figure 6(D)). The mean CNOT7 and CNOT8 content in the N2A cell lysates was 780 ± 63 pg/lane and 815 ± 78 pg/lane respectively, giving a molar ratio close to 1:1. This suggests that CNOT7 outcompetes CNOT8 for binding due to its higher affinity for CNOT1 and not because it is more abundant.

Cnot7 deletion reduces CNOT6 and CNOT6L protein

In addition to their deadenylase function, CNOT7/8 act as a scaffold to recruit the other CCR4-NOT catalytic subunits, CNOT6 and CNOT6L, to the complex.[12] CNOT6 and CNOT6L levels in the hippocampus of *Cnot7*-KO mice were reduced by 39% (P = 0.0002) and 62% (P = 0.0008) respectively (Figure 7(A)). In N2A cells, FLAG-IP showed that FLAG-tagged CNOT7-M141A was able to bind both CNOT6 and CNOT6L as strongly as FLAG-CNOT7-WT (Figure 7(B)), suggesting that the interaction between CNOT7 and CNOT6/6L is not CNOT1-dependent.

In contrast, the interaction between CNOT6L and FLAG-tagged CNOT8-M141A was clearly reduced compared to FLAG-CNOT8-WT (Figure 7(C)), even though levels of FLAG-CNOT8-WT and CNOT8-M141A in FLAG-IP samples were similar. CNOT6 could not be reliably detected in either

Figure 6. CNOT8 protein is stabilized by binding to CCR4-NOT. (A) After 24 hours incubation with 25 μM CHX, FLAG-tagged wild-type CNOT8 shows similar degradation to endogenous CNOT8. CNOT8-M141A (red) was significantly less stable (P = 0.018) than CNOT8-WT (black), suggesting that interaction with CCR4-NOT protects CNOT8 from degradation. Quantification of the band intensity by densitometry is shown. The graph shows mean protein expression relative to 0 h for each protein, normalized to GAPDH; error bars show SEM. **, $p < 0.01$, Student's t-test. (B) FLAG-CNOT7-M141A remained stable. (C) Recombinant FLAG-tagged CNOT1-MIF4G (FLAG-CNOT1-MIF4G) was combined with an excess of CNOT7 and/or CNOT8 and pulled down using anti-FLAG beads. Both CNOT7 and CNOT8 were able to bind to FLAG-CNOT1-MIF4G. When both proteins were present, CNOT8 did not affect the interaction between FLAG-CNOT1-MIF4G and CNOT7 (compare lanes 8 and 10), but CNOT7 reduced CNOT8 binding to background (compare lanes 9 and 10). (D) The mean CNOT7 and CNOT8 content in N2A cell lysates (red; 6.3 μg total protein per lane) was estimated by comparison to a standard curve (blue) made from recombinant human CNOT7 or CNOT8 protein.

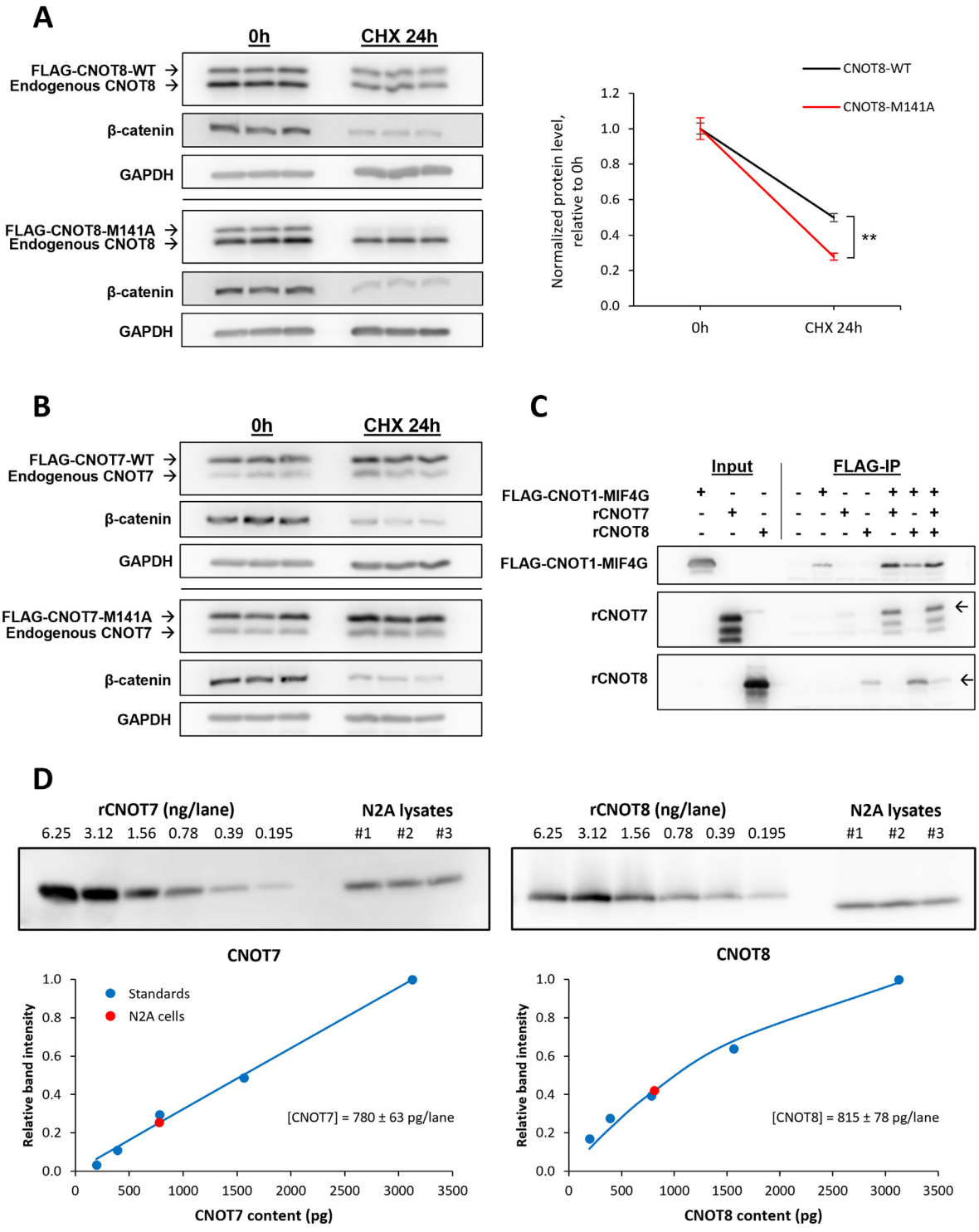
A
0h
CHX 24h
FLAG-CNOT8-WT →
Endogenous CNOT8 →
β-catenin
GAPDH
FLAG-CNOT8-M141A →
Endogenous CNOT8 →
β-catenin
GAPDH
CNOT8-WT
CNOT8-M141A
Normalized protein level, relative to 0h
1.2
1.0
0.8
0.6
0.4
0.2
0.0
**
0h
CHX 24h
B
0h
CHX 24h
FLAG-CNOT7-WT →
Endogenous CNOT7 →
β-catenin
GAPDH
FLAG-CNOT7-M141A →
Endogenous CNOT7 →
β-catenin
GAPDH
C
Input
FLAG-IP
FLAG-CNOT1-MIF4G
rCNOT7
rCNOT8
FLAG-CNOT1-MIF4G
rCNOT7
rCNOT8
D
rCNOT7 (ng/lane)
6.25 3.12 1.56 0.78 0.39 0.195
N2A lysates
#1 #2 #3
rCNOT8 (ng/lane)
6.25 3.12 1.56 0.78 0.39 0.195
N2A lysates
#1 #2 #3
CNOT7
Standards
N2A cells
Relative band intensity
[CNOT7] = 780 ± 63 pg/lane
CNOT7 content (pg)
CNOT8
Relative band intensity
[CNOT8] = 815 ± 78 pg/lane
CNOT8 content (pg)

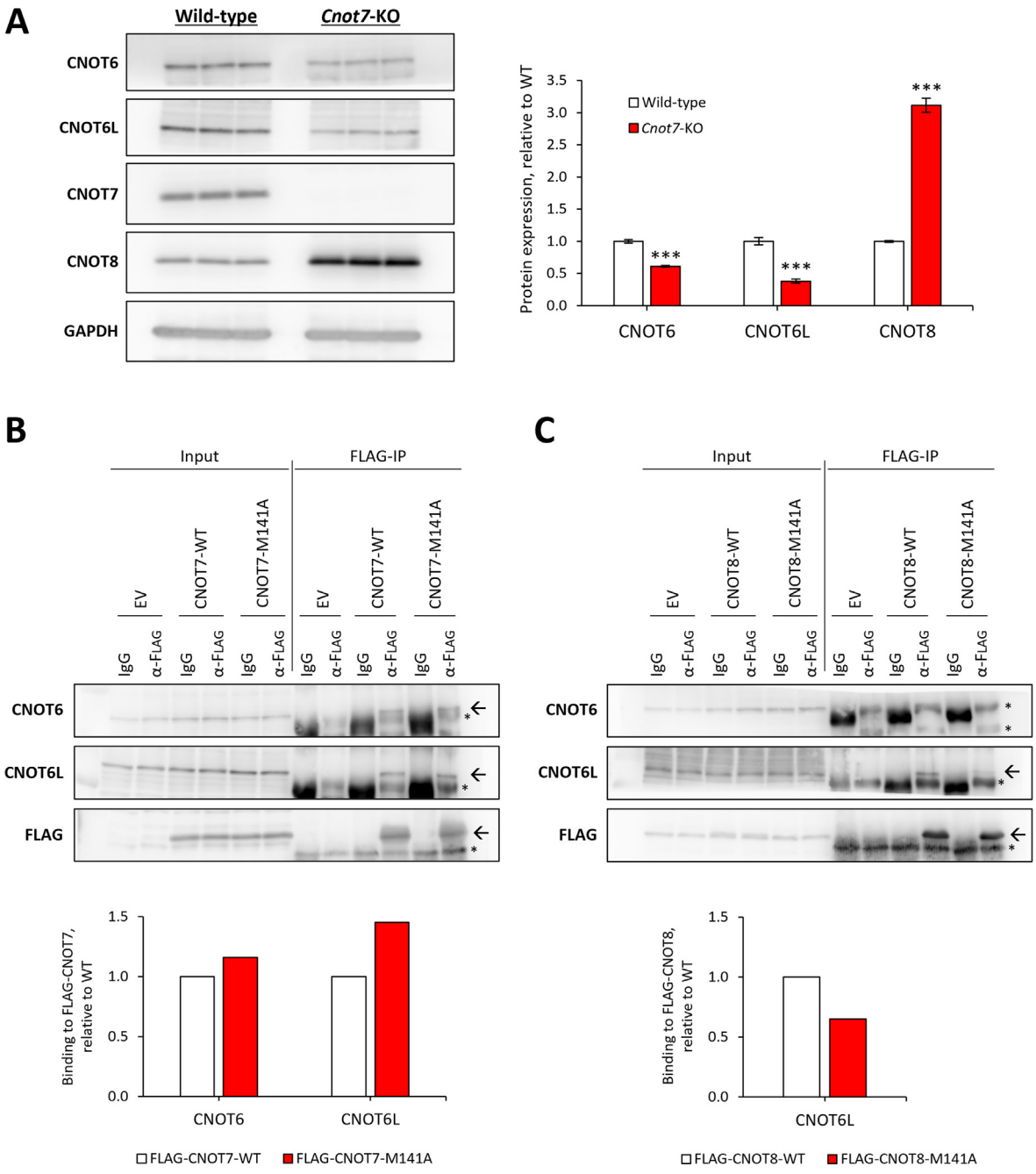

Figure 7. CNOT7 depletion also decreases CNOT6 and CNOT6L. (A) Western blotting shows that CNOT6 and CNOT6L are reduced in the hippocampus of *Cnot7*-KO mice compared to wild-type littermates, even though CNOT8 is increased. Quantification of CNOT6 and CNOT6L in wild-type (white) and *Cnot7*-KO (red) hippocampus by densitometry is shown on the right side. ***, $p < 0.001$; Student's t-test. (B) CNOT6 and CNOT6L interact similarly with CNOT7-WT and CNOT7-M141A. (C) CNOT6L co-immunoprecipitation with CNOT8-M141A was reduced compared to CNOT8-WT, although CNOT8 IP levels appeared similar. CNOT6 was not clearly detected in either FLAG-CNOT8-WT or FLAG-CNOT8-M141A IP samples. Arrows on western blot images indicate specific CNOT6, CNOT6L or FLAG bands; Asterisks (*) indicate non-specific bands. For (B) and (C), the interaction between FLAG-CNOT7/8 and CNOT6/6L was quantified by densitometry from the western blots. Values of the co-IPed protein in CNOT7/8-M141A-expressing cells were normalized to the IPed protein (FLAG) and expressed relative to CNOT7/8-WT-expressing cells.

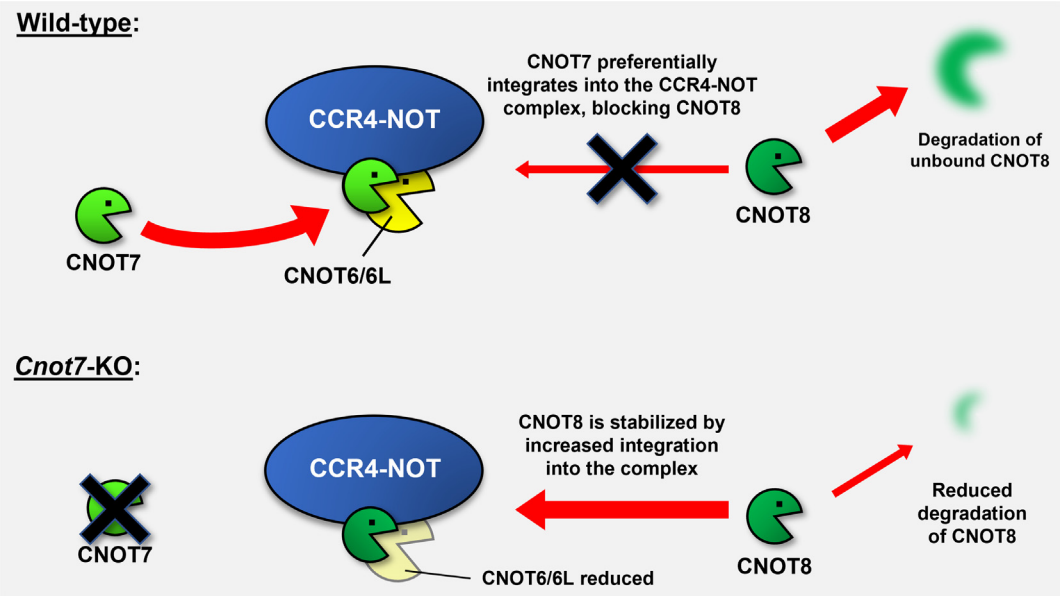

Figure 8. A model of the mechanism by which CNOT8 is increased by CNOT7 depletion. In wild-type cells, CNOT7 preferentially binds to CNOT1 via the MIF4G domain and integrates into the CCR4-NOT complex. CNOT8 is excluded and unbound CNOT8 is degraded by the proteasome. In *Cnot7*-KO tissue, or in CNOT7-depleted cells, CNOT8 can integrate into the CCR4-NOT complex, which stabilizing it and protecting it from degradation. However, the increased integration of CNOT8 into the CCR4-NOT complex fails to fully compensate for loss of CNOT7 in terms of recruiting CNOT6 and CNOT6L due to the weaker interaction between CNOT8 and CNOT6/6L.

wild-type or M141A mutant FLAG-CNOT8 IP samples, suggesting that CNOT8 may not interact strongly with CNOT6 in these cells. These data suggest that increased CNOT8 may not completely compensate for CNOT7 in recruiting CNOT6 and CNOT6L and that binding of CNOT8 to CNOT1 may be required for the efficient interaction between CNOT8 and CNOT6L, perhaps due to stabilization of CNOT8 by CNOT1.

Discussion

We show here that CNOT8 protein is increased by CNOT7 depletion without corresponding changes in *Cnot8* mRNA, suggesting post-transcriptional regulation of CNOT8 expression. Elevated CNOT8 most likely does not result from increased translation, but instead from greater protein stability in the absence of CNOT7. CNOT7 was able to prevent CNOT8 from being incorporated into the CCR4-NOT complex and loss of CNOT7 increased the interaction between CNOT8 and the CCR4-NOT complex. Mutant CNOT8 protein that could not bind the CCR4-NOT scaffold CNOT1 was less stable than wild-type CNOT8, suggesting that interaction with CCR4-NOT may protect CNOT8 from degradation. In contrast, CNOT7 stability was not dependent on binding to CNOT1. This study suggests that CNOT7 is the dominant Caf1 homolog in the mammalian CCR4-NOT complex because of its greater affinity for CNOT1 and highlights distinct characteristics of each homolog (Figure 8).

RIP assays using a CNOT3 antibody identified interactions with the mRNAs encoding all the deadenylase subunits of the CCR4-NOT complex (Figure 2(A)). CNOT3-IP using this antibody has been shown to co-immunoprecipitate other CCR4-NOT subunits, including CNOT1, CNOT2, CNOT6L and CNOT7/8.[8,28] Therefore, these mRNAs may interact with CNOT3 via CCR4-NOT and this raises the possibility that CCR4-NOT might regulate the expression of its own subunits. In particular, depletion of CNOT7 in N2A cells appeared to reduce the co-immunoprecipitation of *Cnot6l* and *Cnot8* mRNAs with CNOT3. It is possible that *Cnot6l* and *Cnot8* mRNAs co-immunoprecipitated with CNOT3 via non-CCR4-NOT proteins such as translating ribosomes,[29] but there is currently no evidence that CNOT7 depletion affects these interactions. The pull-down of these mRNAs was mainly dependent on CNOT7, directly or indirectly, and increased CNOT8 could not fully compensate for loss of CNOT7 in this case. Although *Cnot8* mRNA might be bound by CCR4-NOT, and its co-immunoprecipitation with CNOT3 was dependent on CNOT7, its stability was unaffected by *Cnot7* knockdown. This seems contradictory, but deletion of RNA-binding proteins does not necessarily alter the expression of their targets. For example, the yeast Pumilio homolog Puf3p has been found to interact with over 1000 mRNAs, but less than 10% of these transcripts were increased in ΔPuf3p

mutant cells.[33] In other cell types, or in other contexts, *Cnot8* mRNA stability could be regulated by CCR4-NOT and CNOT7.

The data in Figures 3(B) and (C) suggest that increased CNOT8 protein in CNOT7-depleted N2A cells does not arise from increased translation. However, the first conserved region of the *Cnot8* 3′UTR, ECR1, may affect translation as luciferase activity was reduced in *Cnot7*-KD cells compared to controls when ECR1 was present in the 3′UTR without reducing *FLuc* mRNA (Figure 3(B); Figure S3(C)), indicating suppression of translation. ECR1 contains conserved putative binding sites for the miRNAs miR-7-5p and miR-138-5p, in addition to a potential nanos binding site (UGUA) and another site, UUUUUAA, that closely resembles the neuron-specific RBP HuD/ELAVL4 consensus sequence (Figure 3(A); Figure S2).[30] UUUUUAA is also enriched in the 3′UTRs of AGO-bound mRNAs, and it is associated with regulation of mRNA by miRNA.[34] The presence of miRNA binding sites together with UUUUUAA sites in the 3′UTR suggests that *Cnot8* mRNA stability and translation could be regulated via miRNA/AGO, which is also known to interact with the CCR4-NOT complex.[34–35]

Despite their high similarity (75% similar amino acid sequences; Figure S5(A)), CNOT7 and CNOT8 proteins show markedly different stability (Figure 4(A)), and it is likely that their stability is regulated in different ways. CNOT8 was stabilized by binding to the CCR4-NOT complex (Figure 6(A)), but CNOT7 remained highly stable even when it could not bind to CNOT1 (Figure 6(B)). This suggests that the stability of CNOT8 is at least partly dependent on binding to CNOT1, whereas the increased stability of CNOT7 does not derive only from its higher affinity for CNOT1. A previous study noted that expression of recombinant human CNOT8 was higher when co-expressed with full-length CNOT1 or the MIF4G domain, and the authors hypothesized that the interaction may stabilize CNOT8.[24] The structure of CNOT8 has not been determined experimentally, but it is predicted to be very similar to CNOT7 (Figure S5(B)). The structures of CNOT7 and CNOT8 predicted using AlphaFold2 (alphafold.ebi.ac.uk[35–36]) are very similar to the published experimentally determined structure of CNOT7.[24,37–38] Most of the functionally important residues that have been identified in CNOT7 are conserved in CNOT8 (Figure S5(A)). The CNOT1-binding interface of CNOT7 comprises eight residues (shaded green in Figure S5A[24]) and all of these are conserved in CNOT8 except for the polar uncharged Asn171 (N), which is substituted for a negatively charged Asp (D) residue in CNOT8. The consequences of this are not clear, but N171 in CNOT7 contacts the central Pro1257 in the binding region of the CNOT1 MIF4G domain and its substitution may therefore reduce the strength of the interaction between CNOT8 and CNOT1.

CNOT7/8 play a scaffolding role in CCR4-NOT by recruiting CNOT6 and CNOT6L to the complex. Levels of CNOT6 and CNOT6L were significantly reduced in *Cnot7*-KO brain tissue (Figure 7(A)) and therefore the increased CNOT8 protein in *Cnot7*-KO tissue is not sufficient to maintain CNOT6 and CNOT6L protein levels. *Cnot6* mRNA expression was reduced in *Cnot7*-KD N2A cells (Figure 2(A)), which could result from reduced transcription or from altered mRNA stability. Therefore, the reduction in CNOT6 protein could result from altered transcription, translation, or protein stability. As *Cnot6l* mRNA was not altered in *Cnot7*-KD cells, the reduction in CNOT6L is more likely to be caused by decreased translation or protein stability.

A previous study found that human CNOT8 only bound to CNOT6 under low-salt conditions, whereas CNOT7 remained bound to CNOT6 even in high-salt conditions, suggesting that CNOT6 binds CNOT8 with lower affinity than it binds CNOT7.[12] Moreover, the same study did not detect CNOT6 or CNOT6L by mass spectrometry after co-IP to identify proteins interacting with CNOT8, whereas CNOT6 and CNOT6L did co-IP with CNOT7. In support of this, we clearly detected the interaction between CNOT6 and CNOT7 (Figure 7(B)), but not CNOT8 (Figure 7(C)). The interaction between CNOT6L and CNOT8 was detected, but our data suggest that the recruitment of CNOT6L by CNOT8 is dependent on the interaction between CNOT8 and CNOT1 (Figure 7(C)), perhaps due to stabilization of CNOT8 (Figure 6(A)). Of the residues in CNOT7 that are involved in binding to CNOT6/6L (shaded yellow in Figure S5(A)), three are substituted in CNOT8 (Val48A, N57S and A58I).[16] These substitutions could reduce the affinity of CNOT8 for CNOT6/6L. Binding of CNOT6 and CNOT6L to CNOT7 was not CNOT1-dependent (Figure 7(B)). As CNOT8 is stabilized by binding to CNOT1, it is possible that CNOT7′s stability outside the CCR4-NOT complex could be enhanced by its higher affinity for CNOT6/6L. Currently, little is known about the interactions and possible functions of CNOT7 and CNOT6/6L outside CCR4-NOT.

If, like CNOT8, stability of CNOT6/6L is influenced by their integration into the CCR4-NOT complex, lower affinity binding to CNOT8 in the absence of CNOT7 could contribute to the reduction in their expression. The CCR4-NOT deadenylase subunits have enzymatic activity in isolation,[39–40] but their specificity and activity are enhanced by integration into the complex.[14] In *Cnot7*-KO tissue, reduced CNOT6/6L protein and the potentially lower affinity interaction between CNOT6/6L and CNOT8 may result in the

stabilization of CNOT6/6L target mRNAs in addition to CNOT7 targets. The deadenylase activity of CNOT7 is increased by its incorporation into CCR4-NOT[14] and there is some evidence that the nuclease domain of CNOT6 may somehow contribute to this effect.[16] Therefore, the deadenylase activity of CNOT7 and CNOT8 could differ as a result of their different affinity for CNOT6/6L.

While the core sequence of CNOT7 and CNOT8 is mostly conserved, they differ significantly at their C-termini (Figure S5(A)) and this region may contribute to the differences in stability and protein binding between these paralogous subunits. Structural analyses of human CNOT7 show that the C-terminus lies on the outside of the protein, close to the active site, and is not obscured by binding to the CNOT1-MIF4G domain,[24] CNOT6[38] or TOB1.[37] Deletion of the last 22 residues from the C-terminus of CNOT7 significantly increased the activity of a purified CNOT6-CNOT7 complex in an *in vitro* deadenylation assay,[16] suggesting that it is functional. Short, unstructured C-terminal domains like those in CNOT7/8 have important regulatory functions in other proteins. For example, p53 has an unstructured C-terminal domain of a similar size to that of CNOT8 which is thought to have functions relating to protein stability, co-factor recruitment and DNA binding.[41] The exposed C-termini of CNOT7 and CNOT8 could therefore act as sites for post-translational modification, mediate specific protein–protein interactions, or influence binding of CNOT7/8 to their RNA targets and their subsequent deadenylation.

The stability of CNOT7 protein may indicate a housekeeping role, in which rapid modulation of protein levels is less important. In contrast, the relative instability of both *Cnot8* mRNA (Figure 2(B)) and CNOT8 protein (Figure 4(A)) implies that protein turnover is likely to be much faster for CNOT8 than CNOT7. This could allow levels of CNOT8 protein to be modulated much more rapidly than CNOT7 and may suggest a role for CNOT8 in responding to some as-yet-unidentified stimulus. At present, the factors regulating CNOT8 expression are not well understood. Global deletion of CNOT8 in mice causes embryonic lethality at E9.0–9.5,[6] and in zebrafish, cnot8 may regulate FGF signaling in the brain during embryogenesis.[42] Thus, CNOT8 is likely to have a specific function during embryogenesis which cannot be compensated for by CNOT7. Investigation of the underlying cause of embryonic lethality in *Cnot8* mutant mice would shed light on the distinct physiological functions of CNOT8.

Alternatively, activity of CNOT8 could be regulated at the level of protein expression/degradation, while CNOT7 activity may be regulated more by post-translational modifications such as ubiquitination. For example, the CNOT7-dependent degradation of *MHC-I* mRNA in HEK293T cells was promoted by the ubiquitination of CNOT7 by the RNA-binding E3 ubiquitin ligase MEX-3C.[43] The lysine residues in CNOT7 that may be ubiquitinated by MEX-3C (shaded red in Figure S5(A)) are completely conserved in CNOT8, but the effects of ubiquitination on CNOT8 activity or stability are not known. Components of the CCR4-NOT complex, notably including CNOT8 but not CNOT7, were identified as potential targets of the Skp-Cullin-F-box (SCF)$^{\beta TrCP1/2}$ E3 ubiquitin ligase complex in HEK293-derived cells.[44] Therefore, CNOT7 and CNOT8 may be targeted by different E3 ubiquitin ligases, and this could explain the observed differences in protein stability.

This study sheds light on distinct physiological functions exerted by CNOT7 or CNOT8 by their distinct natures of protein stabilities and affinities with other components of the CCR4-NOT complex.

Materials and methods

Animals

All use of animals was approved by the OIST Animal Care and Use Committee. All mice were on a C57BL/6J background. *Cnot7*-KO mice have been described previously.[3] *Cnot8*-KO is embryonic lethal, so conditional knockout mice were produced by crossing *Cnot8*-flox mice[6] with Tg (Camk2a-cre)2Gsc mice,[25] which express Cre recombinase in a subset of excitatory forebrain neurons under the control of the *Camk2a* promoter.

Cell culture

N2A (Neuro2A) mouse neuroblastoma cells were maintained in Dulbecco's modified Eagle medium (DMEM) containing 10% fetal calf serum (FCS) and penicillin/streptomycin. For transfection, cells were transferred to DMEM containing 5% FCS and no antibiotics. Transfections were performed using RNAiMAX for siRNA or Lipofectamine 3000 for plasmid DNA (both from Invitrogen) according to the manufacturer's protocols. The sequences of the siRNAs used to knockdown *Cnot7* in N2A cells are shown in Table 1. For assessing stability of CNOT7 and CNOT8 proteins, N2A cells were

Table 1 siRNA sequences used for *Cnot7* knockdown in N2A cells.

siRNA	Sense sequence (5′-3′)	Antisense sequence (5′-3′)
Non-targeting control	UUCUCCGAACGUGUCACGUTT	ACGUGACACGUUCGGAGAATT
Cnot7 #1	GACUCUAUAGAGCUACUAACA	UUAGUAGCUCUAUAGAGUCCU
Cnot7 #2	GGUGUAAUGUAGACUUGUUAA	AACAAGUCUACAUUACACCGC

Table 2 Primers used for quantitative PCR.

Gene symbol	RefSeq	Forward primer (5′-3′)	Reverse primer (5′-3′)
Cnot6	NM_001290741.1	TGTATTGGGAGAATGTGGAACT	ACCCCACCAGTGCTCAAATA
Cnot6l	NM_001285511.1	CCTCGCAGAATTTACACCATC	TTAAGCTCCGCACTCTACCC
Cnot7	NM_001271542.1	CCAGGCAGGATCTGACTCAC	TGACCACAGTATTTGGCATCA
Cnot8	NM_026949.3	CATCGGGAGTGGTTCTCTGT	GGCAGGCGAGAGTCTGTTAG
Gapdh	NM_001289726.1	CTGCACCACCAACTGCTTAG	GTCTTCTGGGTGGCAGTGAT
Fluc	-	AGAACTGCCTGCGTGAGATT	AAAACCGTGATGGAATGGAA

treated with 25 μM or 50 μM cycloheximide (Sigma) and 10 μM MG132 (Sigma).

Western blotting

Cells were lysed in TNE buffer (50 mM Tris pH7.5, 150 mM NaCl, 1 mM EDTA, 1% NP-40) containing Protease Inhibitor Cocktail (Nacalai Tesque). Tissue was homogenized in TNE buffer by passing it through a needle 10 times. Cultured cells were lysed in ice-cold TNE buffer. Protein concentration was assessed by bicinchoninic acid (BCA) assay (Pierce). Proteins were separated by polyacrylamide gel electrophoresis, transferred to polyvinylidene difluoride (PVDF) membranes, and blocked in 5% skimmed milk in Tris-buffered saline containing 0.05% Tween-20 (TBST). Membranes were washed in TBST and incubated in primary antibodies diluted in Can Get Signal Solution 1 (Toyobo Co. Ltd) incubated at for 1 hour at room temperature or overnight at 4 °C. After washing, membranes were incubated in appropriate HRP-conjugated secondary antibodies diluted 1:3000 in Can Get Signal Solution 2 or TBST. Proteins were visualized by enhanced chemiluminescence (ECL; Millipore) and imaged using a GE Healthcare ImageQuant LAS 4000. Western blots were quantified by densitometry using ImageJ software (NIH). Expression of proteins of interest was normalized to GAPDH protein.

Antibodies

Mouse monoclonal antibodies against CNOT3, CNOT6L and CNOT8 were produced in collaboration with Bio Matrix Research.[45] Mouse monoclonal antibody against CNOT6 was produced as previously described.[6] CNOT7 monoclonal antibody was obtained from Abnova (clone 2F6; H00029883-M01A). Mouse monoclonal β-catenin antibody was from BD Transduction Laboratories (#610153). For FLAG-immunoprecipitation, we used the mouse monoclonal FLAG M2 antibody from Sigma-Aldrich (F1804). Detection of FLAG-tagged proteins by western blotting used a polyclonal rabbit antibody (PM020; MBL Limited). Rabbit GAPDH antibody was from Cell Signaling Technology (#2118).

Quantitative polymerase chain reaction (qPCR)

Total RNA was extracted from cells and tissue using Isogen II (Nippon Gene) according to the manufacturer's protocol. cDNA was synthesized from 500 ng total RNA using PrimeScript II reverse transcriptase (Takara Bio). qPCR was performed using TB Green Premix Ex Taq (Takara). Primers were designed using PrimerBLAST.[46] Primer sequences are shown in Table 2. qPCR was performed using a ViiA 7 Real-Time PCR System (Applied Biosystems). To ensure that qPCR was quantitative across the range of expression, standard curves and blank controls were run for all primer pairs. Expression of target cDNAs was normalized to *Gapdh* expression. Relative expression analysis was performed in QuantStudio v1.3 software (Applied Biosystems).

Ribonucleoprotein-immunoprecipitation (RIP) assays

N2A cells at 80% confluence were transfected with control or *Cnot7* siRNA in 6 cm dishes. After 24 hours, cells were transferred into 10 cm dishes and incubated for another 24 hours. RIP assays were carried out as previously described.[8] Cells were lysed in 1 ml TNE buffer, containing protease and RNase inhibitors, for 30 minutes at 4 °C, then centrifuged at 20,000 G for 10 minutes. 10 μl of the supernatant was removed to confirm CNOT7 knockdown by western blotting and a further 10 μl was removed as an input sample for qPCR. The remaining lysate was divided into two 500 μl aliquots; 1 μg of anti-CNOT3 antibody was added to one tube and normal mouse IgG (sc-2025; Santa Cruz) was added to the other. Lysates were incubated at 4 °C with gentle agitation for 2 hours. 40 μl of protein G-conjugated Dynabeads (Invitrogen) were then added to each tube and the lysates incubated at 4 °C for 1 hour with agitation. The beads were then washed four times in TNE buffer. 1 ml Isogen II was added to each RIP sample and the corresponding input samples and the RNA extracted. The entire RNA sample was dissolved in 8 μl nuclease-free water and cDNA was synthesized using PrimeScript II. qPCR was performed as described above. *Gapdh* was run for input samples to assess initial levels of each mRNA of interest

and standard curves were run for each set of primers using input cDNA from control siRNA-treated cells. The percentage of mRNA in each RIP sample relative to its corresponding input sample was calculated using the $2^{-\Delta\Delta Ct}$ method.

RNA stability assay

N2A cells at 70–80% confluence were treated with 10 μg/ml actinomycin D and cells were lysed in Isogen II for RNA extraction at timepoints up to 9 hours later. In siRNA-treated cells, actinomycin D was added 48 hours after addition of siRNA. RNA extraction, cDNA synthesis and qPCR were performed as described above. Expression of *Cnot7* and *Cnot8* were normalized to *Gapdh* expression.

Luciferase assays

The 3′UTR of mouse *Cnot8* was amplified from cDNA using Phusion high-fidelity polymerase (New England Biolabs) and cloned into a modified pGL3 vector (Promega) with an additional multiple cloning site immediately downstream of the reporter gene.[8] N2A cells were first transfected at 50% confluence with control or *Cnot7* siRNA. 24 hours after addition of siRNA, medium was replaced and cells were transfected with the constructs containing the *Cnot8* 3′UTR fragments together with renilla-expressing pRL-TK (Promega). The following day, cells were lysed and luciferase assays performed using a Dual-Luciferase Reporter Assay kit (Promega) according to the manufacturer's protocol. Firefly and renilla luciferase activity was measured using a Berthold Technologies Centro XS^3 LB 960 luminometer. Firefly luciferase activity was normalized to renilla activity. RNA extraction from lysates using Isogen II, cDNA synthesis and qPCR were performed as described above. Cell lysates were combined with 2x Laemmli buffer and used directly for western blotting to assess CNOT7 and CNOT8 protein levels.

Polysome fractionation

48 hours after transfection with control or *Cnot7* siRNA, N2A cells were washed in ice-cold PBS containing 100 μg/ml cycloheximide and RNase inhibitor, then scraped into 1 ml cold PBS and transferred to a cooled 1.5 ml tube. The cells were spun down and resuspended in hypotonic buffer (5 mM Tris, pH7.6, 1.5 mM KCl, 50 mM MgCl2, containing protease inhibitors, 100 μg/ml cycloheximide, dithiothreitol, RNase inhibitor, Triton X-100 and sodium deoxycholate). The RNA concentration of each lysate was measured using the absorbance at 260 nm and the concentration in each sample equalized by adding additional hypotonic buffer. 50 μl of each lysate was removed and used for qPCR to confirm *Cnot7* knockdown. Lysates were separated by density on a 10–50% sucrose gradient by centrifugation and the sucrose was divided into 12 fractions using a piston gradient fractionator.

RNA distribution was by measuring absorbance at 254 nm of each fraction. RNA was extracted from each fraction and cDNA synthesized from 500 ng RNA using PrimeScript II. qPCR for *Cnot8* was performed as described above. Levels of *Cnot8* mRNA in each fraction were normalized to total mRNA. The total area under the curve was normalized between different samples to analyze the distribution.

Immunoprecipitation

N2A cells or brain tissues were homogenized in 1 ml TNE buffer containing, protease inhibitors, RNase A (10 μg/ml; Sigma) and benzonase (250 units/ml; Millipore). Homogenized samples were incubated on ice for 30 minutes, then cleared by centrifugation at 18,000g for 10 minutes. 25 μl (5%) of the cleared lysate was taken from the lysate as an input sample and mixed with 25 μl 2x Laemmli buffer. Lysates were incubated with 1 μg/ml anti-CNOT3 antibody, anti-CNOT8 antibody, anti-FLAG (M2; Sigma-Aldrich), or a normal mouse IgG control (Santa Cruz) for 2 hours at 4 °C with agitation. Protein G-conjugated Dynabeads (Invitrogen) for 1 hour at 4 °C with gentle mixing. Beads were then washed four times in 400 μl ice-cold TNE buffer. Bead were resuspended in 50 μl 1x Laemmli buffer, heated to 95 °C for 5 minutes, and the beads removed. 20 ul of each sample was used per gel for western blotting.

Recombinant protein purification

cDNAs encoding the MIF4G domain of human CNOT1 (amino acids 1075–1317;[24] with an N-terminal FLAG tag and full-length human CNOT7 were cloned into pGEX-6P-1 (GE Healthcare) to allow expression of an N-terminal glutathione-S-transferase (GST)-tagged fusion protein. BL21-CodonPlus (DE3)-RIPL competent cells (Agilent) were transformed with the construct and grown at 25 °C. Expression of GST-tagged proteins was induced with isopropyl β-D-1-thiogalactopyranoside (IPTG) for 2 hours. Cells were collected by centrifugation and resuspended in PBS, pH7.4, containing 0.1% Triton X-100, 100 μg/ml Lysozyme, 0.05% β-mercaptoethanol, and protease inhibitors, then lysed by sonication. The lysate was centrifuged, and the supernatant was incubated overnight at 4 °C with Glutathione Sepharose 4B beads (GE Healthcare). After washing the beads with PBS containing 0.1% Triton X-100, the recombinant proteins were eluted from the beads using PreScission protease (GE Healthcare) in 50 mM Tris, pH7.0, 150 mM NaCl, 1 mM EDTA, 1 mM DTT, 0.01% Triton-X-100. Isolated recombinant proteins were transferred by dialysis into 20 mM HEPES, pH8.0, 50 mM NaCl, 200 μM

EDTA, 1 mM DTT, 10% glycerol and stored at −80 °C. Protein molecular weight was confirmed by western blotting and concentration was assessed by BCA assay.

In vitro pull-down assay

10 μl protein G-conjugated Dynabeads were washed in ice-cold TNE buffer containing protease inhibitors and resuspended in 150 μl cold TNE. 500 ng anti-FLAG antibody (M2; Sigma-Aldrich) and 100 ng recombinant FLAG-tagged human CNOT1-MIF4G were added and the tube was gently mixed at 4 °C for 1 hour. The beads were then washed twice in 200 μl TNE buffer and resuspended in 150 μl fresh TNE buffer. 200 ng recombinant human CNOT7 and/or CNOT8 protein (both with N-terminal His-tag; Novus Biologicals) were added and the tube was mixed at 4 °C for 1 hour. The beads were washed four times in 200 μl cold TNE buffer then resuspended in 75 μl 1x Laemmli buffer. Samples were denatured at 95 °C for 5 minutes and the beads removed. For input samples, 100 ng recombinant protein was diluted in 75 μl 1x Laemmli buffer. 20 μl of each sample was used per lane for western blotting.

CRediT authorship contribution statement

Patrick N. Stoney: Conceptualization, Methodology, Validation, Formal analysis, Investigation, Resources, Writing – original draft, Writing – review & editing, Visualization, Project administration. **Akiko Yanagiya:** Methodology, Investigation, Resources, Writing – review & editing. **Saori Nishijima:** Investigation. **Tadashi Yamamoto:** Methodology, Resources, Writing – review & editing, Supervision, Project administration, Funding acquisition.

Acknowledgements

This work was supported by the Okinawa Institute of Science and Technology (OIST) subsidiary budget to TY. PS was supported by a Grant-in-Aid for Young Scientist (18K16218) from the Japan Ministry of Education, Culture, Sports, Science and Technology (MEXT). AY was supported by a Grant-in-Aid for Scientific Research (C) (18K06975) and a Grant-in-Aid for Scientific Research in Innovative Areas (20H05351) from MEXT.

Declaration of Competing Interest

The authors declare that they have no known competing financial interests or personal relationships that could have appeared to influence the work reported in this paper.

Appendix A. Supplementary data

Supplementary data to this article can be found online at https://doi.org/10.1016/j.jmb.2022.167523.

Received 11 November 2021;
Accepted 28 February 2022;
Available online 3 March 2022

Keywords:
deadenylase;
deadenylation;
mRNA stability;
protein stability;
CNOT1 scaffold

References

1. Collart, M.A., (2016). The Ccr4-Not complex is a key regulator of eukaryotic gene expression, Wiley Interdisciplinary Reviews. *RNA* **7**, 438–454. https://doi.org/10.1002/wrna.1332.
2. Parker, R., Song, H., (2004). The enzymes and control of eukaryotic mRNA turnover. *Nat. Struct. Mol. Biol.* **11**, 121–127. https://doi.org/10.1038/NSMB724.
3. Nakamura, T., Yao, R., Ogawa, T., Suzuki, T., Ito, C., Tsunekawa, N., Inoue, K., Ajima, R., Miyasaka, T., Yoshida, Y., Ogura, A., Toshimori, K., Noce, T., Yamamoto, T., Noda, T., (2004). Oligo-asthenoteratozoospermia in mice lacking Cnot7, a regulator of retinoid X receptor beta. *Nat. Genet.* **36**, 528–533. https://doi.org/10.1038/ng1344.
4. Cooke, A., Prigge, A., Wickens, M., (2010). Translational repression by deadenylases. *J. Biol. Chem.* **285**, 28506–28513. https://doi.org/10.1074/jbc.M110.150763.
5. Neely, G.G., Kuba, K., Cammarato, A., Isobe, K., Amann, S., Zhang, L., Murata, M., Elmén, L., Gupta, V., Arora, S., Sarangi, R., Dan, D., Fujisawa, S., Usami, T., Ping Xia, C., Keene, A.C., Alayari, N.N., Yamakawa, H., Elling, U., Berger, C., Novatchkova, M., Koglgruber, R., Fukuda, K., Nishina, H., Isobe, M., Pospisilik, J.A., Imai, Y., Pfeufer, A., Hicks, A.A., Pramstaller, P.P., Subramaniam, S., Kimura, A., Ocorr, K., Bodmer, R., Penninger, J.M., (2010). A Global In Vivo Drosophila RNAi Screen Identifies NOT3 as a Conserved Regulator of Heart Function. *Cell* **141**, 142–153. https://doi.org/10.1016/j.cell.2010.02.023.
6. Mostafa, D., Takahashi, A., Yanagiya, A., Yamaguchi, T., Abe, T., Kureha, T., Kuba, K., Kanegae, Y., Furuta, Y., Yamamoto, T., Suzuki, T., (2020). Essential functions of the CNOT7/8 catalytic subunits of the CCR4-NOT complex in mRNA regulation and cell viability. *RNA Biol.* **17**, 403–416. https://doi.org/10.1080/15476286.2019.1709747.
7. Morita, M., Oike, Y., Nagashima, T., Kadomatsu, T., Tabata, M., Suzuki, T., Nakamura, T., Yoshida, N., Okada, M., Yamamoto, T., (2011). Obesity resistance and increased hepatic expression of catabolism-related mRNAs in Cnot3 +/- mice. *EMBO J.* **30**, 4678–4691. https://doi.org/10.1038/emboj.2011.320.
8. Takahashi, A., Adachi, S., Morita, M., Tokumasu, M., Natsume, T., Suzuki, T., Yamamoto, T., (2015). Post-transcriptional Stabilization of Ucp1 mRNA Protects Mice from Diet-Induced Obesity. *Cell Rep.* **13**, 2756–2767. https://doi.org/10.1016/j.celrep.2015.11.056.

9. Mostafa, D., Yanagiya, A., Georgiadou, E., Wu, Y., Stylianides, T., Rutter, G.A., Suzuki, T., Yamamoto, T., (2020). Loss of β-cell identity and diabetic phenotype in mice caused by disruption of CNOT3-dependent mRNA deadenylation. *Commun. Biol.* **3** https://doi.org/10.1038/s42003-020-01201-y.
10. R.K.C. Yuen, D. Merico, M. Bookman, J.L. Howe, B. Thiruvahindrapuram, R.V. Patel, J. Whitney, N. Deflaux, J. Bingham, Z. Wang, G. Pellecchia, J.A. Buchanan, S. Walker, C.R. Marshall, M. Uddin, M. Zarrei, E. Deneault, L. D'Abate, A.J.S. Chan, S. Koyanagi, T. Paton, S.L. Pereira, N. Hoang, W. Engchuan, E.J. Higginbotham, K. Ho, S. Lamoureux, W. Li, J.R. MacDonald, T. Nalpathamkalam, W.W.L. Sung, F.J. Tsoi, J. Wei, L. Xu, A.M. Tasse, E. Kirby, W. van Etten, S. Twigger, W. Roberts, I. Drmic, S. Jilderda, B.M. Modi, B. Kellam, M. Szego, C. Cytrynbaum, R. Weksberg, L. Zwaigenbaum, M. Woodbury-Smith, J. Brian, L. Senman, A. Iaboni, K. Doyle-Thomas, A. Thompson, C. Chrysler, J. Leef, T. Savion-Lemieux, I.M. Smith, X. Liu, R. Nicolson, V. Seifer, A. Fedele, E.H. Cook, S. Dager, A. Estes, L. Gallagher, B.A. Malow, J.R. Parr, S. J. Spence, J. Vorstman, B.J. Frey, J.T. Robinson, L.J. Strug, B.A. Fernandez, M. Elsabbagh, M.T. Carter, J. Hallmayer, B.M. Knoppers, E. Anagnostou, P. Szatmari, R. H. Ring, D. Glazer, M.T. Pletcher, S.W. Scherer, Whole genome sequencing resource identifies 18 new candidate genes for autism spectrum disorder, Nat. Neurosci. 20 (2017) 602–611. https://doi.org/10.1038/nn.4524.
11. Vissers, L.E.L.M., Kalvakuri, S., de Boer, E., Geuer, S., Oud, M., van Outersterp, I., Kwint, M., Witmond, M., Kersten, S., Polla, D.L., Weijers, D., Begtrup, A., McWalter, K., Ruiz, A., Gabau, E., Morton, J.E.V., Griffith, C., Weiss, K., Gamble, C., Bartley, J., Vernon, H.J., Brunet, K., Ruivenkamp, C., Kant, S.G., Kruszka, P., Larson, A., Afenjar, A., Billette de Villemeur, T., Nugent, K., Raymond, F.L., Venselaar, H., Demurger, F., Soler-Alfonso, C., Li, D., Bhoj, E., Hayes, I., Hamilton, N.P., Ahmad, A., Fisher, R., van den Born, M., Willems, M., Sorlin, A., Delanne, J., Moutton, S., Christophe, P., Mau-Them, F.T., Vitobello, A., Goel, H., Massingham, L., Phornphutkul, C., Schwab, J., Keren, B., Charles, P., Vreeburg, M., de Simone, L., Hoganson, G., Iascone, M., Milani, D., Evenepoel, L., Revencu, N., Ward, D.I., Burns, K., Krantz, I., Raible, S.E., Murrell, J.R., Wood, K., Cho, M.T., van Bokhoven, H., Muenke, M., Kleefstra, T., Bodmer, R., de Brouwer, A.P. M., (2020). De Novo Variants in CNOT1, a Central Component of the CCR4-NOT Complex Involved in Gene Expression and RNA and Protein Stability, Cause Neurodevelopmental Delay. *Am. J. Hum. Genet.* **107**, 164–172. https://doi.org/10.1016/j.ajhg.2020.05.017.
12. Lau, N.C., Kolkman, A., van Schaik, F.M.A., Mulder, K.W., Pijnappel, W.W.W.P., Heck, A.J.R., Timmers, H.T.M., (2009). Human Ccr4-Not complexes contain variable deadenylase subunits. *Biochem. J* **422**, 443–453. https://doi.org/10.1042/BJ20090500.
13. Temme, C., Zhang, L., Kremmer, E., Ihling, C., Chartier, A., Sinz, A., Simonelig, M., Wahle, E., (2010). Subunits of the Drosophila CCR4-NOT complex and their roles in mRNA deadenylation. *RNA* **16**, 1356–1370. https://doi.org/10.1261/rna.2145110.
14. Raisch, T., te Chang, C., Levdansky, Y., Muthukumar, S., Raunser, S., Valkov, E., (2019). Reconstitution of recombinant human CCR4-NOT reveals molecular insights into regulated deadenylation. *Nat. Commun.* **10**, 1–14. https://doi.org/10.1038/s41467-019-11094-z.
15. Yi, H., Park, J., Ha, M., Lim, J., Chang, H., Kim, V.N., (2018). PABP Cooperates with the CCR4-NOT Complex to Promote mRNA Deadenylation and Block Precocious Decay. *Mol. Cell* **70**, 1081–1088.e5. https://doi.org/10.1016/j.molcel.2018.05.009.
16. Chen, Y., Khazina, E., Izaurralde, E., Weichenrieder, O., (2021). Crystal structure and functional properties of the human CCR4-CAF1 deadenylase complex. *Nucleic Acids Res.* **49**, 6489–6510. https://doi.org/10.1093/NAR/GKAB414.
17. Aslam, A., Mittal, S., Koch, F., Andrau, J.C., Sebastiaan Winkler, G., (2009). The Ccr4-not deadenylase subunits CNOT7 and CNOT8 have overlapping roles and modulate cell proliferation. *Mol. Biol. Cell* **20**, 3840–3850. https://doi.org/10.1091/mbc.E09-02-0146.
18. Berthet, C., Morera, A.-M., Asensio, M.-J., Chauvin, M.-A., Morel, A.-P., Dijoud, F., Magaud, J.-P., Durand, P., Rouault, J.-P., (2004). CCR4-associated factor CAF1 is an essential factor for spermatogenesis. *Mol. Cell. Biol.* **24**, 5808–5820. https://doi.org/10.1128/MCB.24.13.5808-5820.2004.
19. Washio-Oikawa, K., Nakamura, T., Usui, M., Yoneda, M., Ezura, Y., Ishikawa, I., Nakashima, K., Noda, T., Yamamoto, T., Noda, M., (2007). Cnot7-null mice exhibit high bone mass phenotype and modulation of BMP actions. *J. Bone Mineral Res.* **22**, 1217–1223. https://doi.org/10.1359/jbmr.070411.
20. Bianchin, C., Mauxion, F., Sentis, S., Séraphin, B., Corbo, L., (2005). Conservation of the deadenylase activity of proteins of the Caf1 family in human. *RNA* **11**, 487–494.
21. Youn, J.-Y., Dunham, W.H., Hong, S.J., Knight, J.D.R., Bashkurov, M., Chen, G.I., Bagci, H., Rathod, B., MacLeod, G., Eng, S.W.M., Angers, S., Morris, Q., Fabian, M., Côté, J.-F., Gingras, A.-C., (2018). High-Density Proximity Mapping Reveals the Subcellular Organization of mRNA-Associated Granules and Bodies. *Mol. Cell* **69**, 517–532.e11. https://doi.org/10.1016/j.molcel.2017.12.020.
22. Waghray, S., Williams, C., Coon, J.J., Wickens, M., (2015). Xenopus CAF1 requires NOT1-mediated interaction with 4E-T to repress translation in vivo. *RNA* **21**, 1335–1345. https://doi.org/10.1261/rna.051565.115.
23. Morel, A.P., Sentis, S., Bianchin, C., le Romancer, M., Jonard, L., Rostan, M.C., Rimokh, R., Corbo, L., (2003). BTG2 antiproliferative protein interacts with the human CCR4 complex existing in vivo in three cell-cycle-regulated forms. *J. Cell Sci.* **116**, 2929–2936. https://doi.org/10.1242/jcs.00480.
24. Petit, A.P., Wohlbold, L., Bawankar, P., Huntzinger, E., Schmidt, S., Izaurralde, E., Weichenrieder, O., (2012). The structural basis for the interaction between the CAF1 nuclease and the NOT1 scaffold of the human CCR4-NOT deadenylase complex. *Nucleic Acids Res.* **40**, 11058–11072. https://doi.org/10.1093/nar/gks883.
25. Casanova, E., Fehsenfeld, S., Mantamadiotis, T., Lemberger, T., Greiner, E., Stewart, A.F., Schütz, G., (2001). A CamKIIα iCre BAC allows brain-specific gene inactivation. *Genesis.* **31** https://doi.org/10.1002/gene.1078.
26. Wang, X., Zhang, C., Szábo, G., Sun, Q.Q., (2013). Distribution of CaMKIIα expression in the brain in vivo,

studied by CaMKIIα-GFP mice. *Brain Res.* **1518**, 9. https://doi.org/10.1016/J.BRAINRES.2013.04.042.
27. Cao, M., Wu, J.I., (2015). Camk2a-Cre-mediated conditional deletion of chromatin remodeler Brg1 causes perinatal hydrocephalus. *Neurosci. Lett.* **597**, 71–76. https://doi.org/10.1016/J.NEULET.2015.04.041.
28. Suzuki, T., Kikuguchi, C., Nishijima, S., Nagashima, T., Takahashi, A., Okada, M., Yamamoto, T., (2019). Postnatal liver functional maturation requires Cnot complex-mediated decay of mRNAs encoding cell cycle and immature liver genes. *Development (Cambridge, England)* **146** https://doi.org/10.1242/DEV.168146.
29. Buschauer, R., Matsuo, Y., Sugiyama, T., Chen, Y.H., Alhusaini, N., Sweet, T., Ikeuchi, K., Cheng, J., Matsuki, Y., Nobuta, R., Gilmozzi, A., Berninghausen, O., Tesina, P., Becker, T., Coller, J., Inada, T., Beckmann, R., (2020). The Ccr4-Not complex monitors the translating ribosome for codon optimality. *Science (New York, N.Y.)* **368** https://doi.org/10.1126/SCIENCE.AAY6912.
30. Ashworth, W., Stoney, P.N., Yamamoto, T., (2019). States of decay: The systems biology of mRNA stability. *Curr. Opin. Syst. Biol.* **15**, 48–57. https://doi.org/10.1016/j.coisb.2019.03.006.
31. Ovcharenko, I., Nobrega, M.A., Loots, G.G., Stubbs, L., Browser, E.C.R., (2004). A tool for visualizing and accessing data from comparisons of multiple vertebrate genomes. *Nucleic Acids Res.* **32**, W280. https://doi.org/10.1093/nar/gkh355.
32. Agarwal, V., Bell, G.W., Nam, J.W., Bartel, D.P., (2015). Predicting effective microRNA target sites in mammalian mRNAs. *ELife.* **4** https://doi.org/10.7554/eLife.05005.
33. Kershaw, C.J., Costello, J.L., Talavera, D., Rowe, W., Castelli, L.M., Sims, P.F.G., Grant, C.M., Ashe, M.P., Hubbard, S.J., Pavitt, G.D., (2015). Integrated multi-omics analyses reveal the pleiotropic nature of the control of gene expression by Puf3p. *Sci. Rep.* **5**, 15518. https://doi.org/10.1038/srep15518.
34. Jacobsen, A., Wen, J., Marks, D.S., Krogh, A., (2010). Signatures of RNA binding proteins globally coupled to effective microRNA target sites. *Genome Res.* **20**, 1010–1019. https://doi.org/10.1101/gr.103259.109.
35. J. Jumper, R. Evans, A. Pritzel, T. Green, M. Figurnov, O. Ronneberger, K. Tunyasuvunakool, R. Bates, A. Žídek, A. Potapenko, A. Bridgland, C. Meyer, S.A.A. Kohl, A.J. Ballard, A. Cowie, B. Romera-Paredes, S. Nikolov, R. Jain, J. Adler, T. Back, S. Petersen, D. Reiman, E. Clancy, M. Zielinski, M. Steinegger, M. Pacholska, T. Berghammer, S. Bodenstein, D. Silver, O. Vinyals, A.W. Senior, K. Kavukcuoglu, P. Kohli, D. Hassabis, Highly accurate protein structure prediction with AlphaFold, Nature 2021 596:7873. 596 (2021) 583–589. https://doi.org/10.1038/s41586-021-03819-2.
36. Varadi, M., Anyango, S., Deshpande, M., Nair, S., Natassia, C., Yordanova, G., Yuan, D., Stroe, O., Wood, G., Laydon, A., Žídek, A., Green, T., Tunyasuvunakool, K., Petersen, S., Jumper, J., Clancy, E., Green, R., Vora, A., Lutfi, M., Figurnov, M., Cowie, A., Hobbs, N., Kohli, P., Kleywegt, G., Birney, E., Hassabis, D., Velankar, S., (2022). AlphaFold Protein Structure Database: massively expanding the structural coverage of protein-sequence space with high-accuracy models. *Nucleic Acids Res.* **50**, D439–D444. https://doi.org/10.1093/NAR/GKAB1061.
37. Horiuchi, M., Takeuchi, K., Noda, N., Muroya, N., Suzuki, T., Nakamura, T., Kawamura-Tsuzuku, J., Takahasi, K., Yamamoto, T., Inagaki, F., (2009). Structural basis for the antiproliferative activity of the Tob-hCaf1 complex. *J. Biol. Chem.* **284**, 13244–13255. https://doi.org/10.1074/JBC.M809250200.
38. Winkler, G.S., Balacco, D.L., (2013). Heterogeneity and complexity within the nuclease module of the Ccr4-Not complex. *Front. Genetics* **4**, 296. http://www.ncbi.nlm.nih.gov/pubmed/24391663 (accessed July 29, 2021).
39. Wang, H., Morita, M., Yang, X., Suzuki, T., Yang, W., Wang, J., Ito, K., Wang, Q., Zhao, C., Bartlam, M., Yamamoto, T., Rao, Z., (2010). Crystal structure of the human CNOT6L nuclease domain reveals strict poly(A) substrate specificity. *EMBO J.* **29**, 2566–2576. https://doi.org/10.1038/emboj.2010.152.
40. Viswanathan, P., Ohn, T., Chiang, Y.C., Chen, J., Denis, C. L., (2004). Mouse CAF1 can function as a processive deadenylase/3′-5′ -exonuclease in vitro but in yeast the deadenylase function of CAF1 is not required for mRNA poly(A) removal. *J. Biol. Chem.* **279**, 23988–23995. https://doi.org/10.1074/jbc.M402803200.
41. Laptenko, O., Tong, D.R., Manfredi, J., Prives, C., (2016). The Tail That Wags the Dog: How the Disordered C-Terminal Domain Controls the Transcriptional Activities of the p53 Tumor-Suppressor Protein. *Trends Biochem. Sci.* **41** https://doi.org/10.1016/j.tibs.2016.08.011.
42. Koch, P., Löhr, H.B., Driever, W., (2014). A Mutation in cnot8, Component of the Ccr4-Not Complex Regulating Transcript Stability, Affects Expression Levels of Developmental Regulators and Reveals a Role of Fgf3 in Development of Caudal Hypothalamic Dopaminergic Neurons. *PLoS ONE* **9**, https://doi.org/10.1371/journal.pone.0113829 e113829.
43. Cano, F., Rapiteanu, R., Winkler, G.S., Lehner, P.J., (2015). A non-proteolytic role for ubiquitin in deadenylation of MHC-I mRNA by the RNA-binding E3-ligase MEX-3C. *Nat. Commun.* **6**, 1–8. https://doi.org/10.1038/ncomms9670.
44. Coyaud, E., Mis, M., Laurent, E.M.N., Dunham, W.H., Couzens, A.L., Robitaille, M., Gingras, A.C., Angers, S., Raught, B., (2015). BioID-based Identification of Skp Cullin F-box (SCF)β-TrCP1/2 E3 Ligase Substrates. *Mol. Cell. Proteomics* **14**, 1781–1795. https://doi.org/10.1074/MCP.M114.045658.
45. Suzuki, T., Kikuguchi, C., Sharma, S., Sasaki, T., Tokumasu, M., Adachi, S., Natsume, T., Kanegae, Y., Yamamoto, T., (2015). CNOT3 suppression promotes necroptosis by stabilizing mRNAs for cell death-inducing proteins. *Sci. Rep.* **5**, 1–14. https://doi.org/10.1038/srep14779.
46. Ye, J., Coulouris, G., Zaretskaya, I., Cutcutache, I., Rozen, S., Madden, T.L., (2012). Primer-BLAST: a tool to design target-specific primers for polymerase chain reaction. *BMC Bioinf.* **13**, 134. https://doi.org/10.1186/1471-2105-13-134.